

Supporting Information

Table of Contents

Table of Contents.....	1
Materials and Methods	2
Synthetic Procedures	3
X-Ray analysis.....	8
NMR Spectra	9
MS Spectra	26
UV-Vis spectra of 3	28
Cyclic Voltammetry	28
DFT calculations.....	29
References	30

Supporting Information

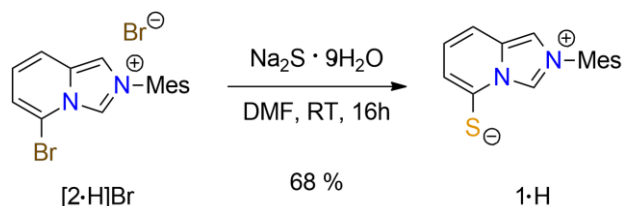
Materials and Methods

All manipulations were performed under an inert atmosphere of dry nitrogen by using standard vacuum line and Schlenk tube techniques or in a dry, oxygen-free and nitrogen filled glovebox. Dry and oxygen-free organic solvents (THF, Et₂O, CH₂Cl₂, toluene, pentane) were obtained using LabSolv (Innovative Technology) solvent purification system. Alternatively, solvents were dried manually prior to distillation under an inert atmosphere of dry nitrogen using Na/benzophenone (THF, Et₂O) or CaH₂ (CH₂Cl₂, C₂H₄Cl₂) as the drying agents. DMF was degassed by bubbling N₂ for 15 min and was stored over activated 4 Å molecular sieves. [2•H]Br¹ and NiCl₂(dme)² were synthesized according to literature procedures. All other reagent-grade chemicals were purchased from commercial sources and used as received. Chromatographic purification of the compounds was performed on silica gel (SiO₂, 63–200 μm). ¹H, ¹³C, and ¹⁹F NMR spectra were obtained on Bruker Avance 400, Avance III HD400, or Avance 500 spectrometers and were referenced relative to the residual signals of the deuterated solvents (¹H and ¹³C) and to CFCl₃ (¹⁹F, external standard).³ Chemical shifts were reported in ppm. ¹H and ¹³C NMR signals were assigned by means of additional ¹³C{¹H}, ¹³C-DEPT135, ¹H-¹H COSY, ¹H-¹³C HMQC, HSQC, and/or HMBC experiments. Mass spectrometry was performed either by the mass spectrometry service of the “Institut de chimie de Toulouse” using a Xevo G2 QToF (Waters) spectrometer (ESI-TOF MS) and timsTOF Flex (Bruker) (MALDI-TOF MS) or by the chromatography service at the “Instituto de Química” (UNAM, Mexico) using a LC-MS system consisting of an Agilent Model 1200 liquid chromatograph coupled to a Bruker Esquire 6000 mass spectrometer (ESI ion trap MS) and a Bruker Microflex spectrometer (MALDI-TOF MS). Elemental analyses were carried out by the elemental analysis service of the LCC (Toulouse, France) using a PerkinElmer 2400 series II analyzer. X-band EPR spectrum was recorded using Elexsys ESP 500 spectrometer. Landé factors were measured by comparison with a reference DPPH sample (g = 2.0036). The numerical simulation of EPR spectra was performed using EasySpin software.⁴ The bulk purity of all new compounds was established by NMR spectroscopy and elemental analysis.

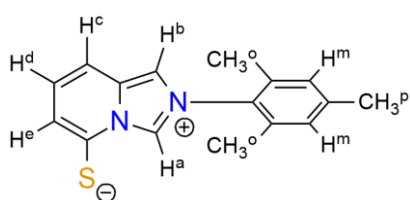
Supporting Information

Synthetic Procedures

Preparation of 1·H



$Na_2S \cdot 9 H_2O$ (2.40 g, 10.0 mmol) was weighed in a 250 mL round-bottom Schlenk flask and dried under vacuum. DMF (100 mL, stored over molecular sieves under N_2 atmosphere) was added under N_2 flow, which partly dissolved the solid, resulting in a light blue solution. $[2\cdot H]Br$ (1.98 g, 5.0 mmol) was added directly as a solid under N_2 flow, followed by an immediate color change to intense green that slowly changed to yellow while stirring the reaction mixture, and formation of a colorless precipitate was observed. After stirring at room temperature for 16 h, the solvent was removed by evaporation in vacuo. The residue was redissolved in EtOAc and filtered through a Celite pad to separate the salt that formed during the reaction. The Celite pad was washed with EtOAc until the filtrate became colorless. The filtrate was then washed 3 times with distilled H_2O to remove traces of DMF, dried over Na_2SO_4 , filtered, and the solvent was removed under reduced pressure. The brown residue was purified by column chromatography (silica gel, hexane/EtOAc gradient from 2:1 to 1:4) yielding 0.91 g (3.4 mmol, 68 %) of a yellow solid. Single crystals suitable for X ray diffraction analysis were obtained by vapor diffusion of diethylether into a concentrated solution of the product in CH_2Cl_2 .

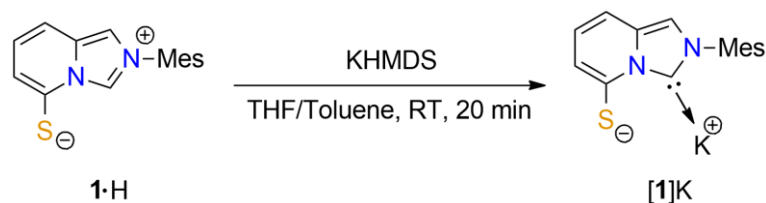


1H NMR ($CDCl_3$, 300 MHz): δ (ppm) = 9.56 (dd, $J = 2.2$ Hz, 0.8 Hz, 1H, H^a), 7.26 (d, $J = 2.2$ Hz, 1H, H^b), 7.16 (dd, $J = 7.0$, 1.5 Hz, 1H, H^d), 7.10 - 7.00 (m, 4H, H^c , H^e , H^m), 2.38 (s, 3H, CH_3 para), 2.02 (s, 6H, CH_3 ortho). $^{13}C\{^1H\}$ NMR ($CDCl_3$, 75 MHz): δ (ppm) = 153.3 (C-S), 141.0 (C_{o-Mes}), 134.2 (C_{p-Mes}),

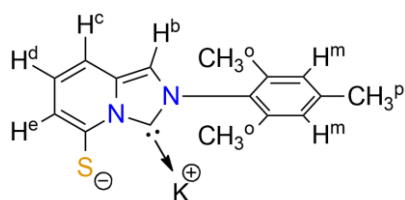
132.9 ($C_{ipso-Mes}$), 131.9 (C_{imPy}), 129.6 (C- H^m Mes), 127.5 (C- H^c), 125.3 (C- H^a), 117.8 (C- H^d), 111.0 (C- H^b), 104.2 (C- H^e), 21.1 (CH_3 para), 17.1 (CH_3 ortho). HR-MS (ESI-TOF): m/z : calc. for $C_{16}H_{17}N_2S$ ($M+H^+$): 269.1112; found: 269.1114, $\epsilon_r = 0.7$ ppm. Elemental analysis: calc. for $C_{16}H_{16}N_2S$: C 71.61 %, H 6.01 %, N 10.44 %; found: C 71.66 %, H 5.93 %, N 10.47 %.

Supporting Information

Preparation of [1]K

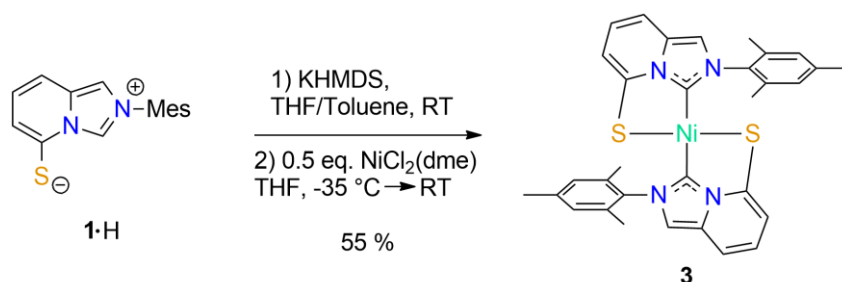


1-H (268 mg, 1.00 mmol) was weighed into a Schlenk flask and cycled 3 times before 20 mL dry THF were added under N₂ flow. 2.2 mL (1.10 mmol) of a 0.5 M solution of KHMDS in toluene were added dropwise to the yellow solution resulting in a color change to dark brown. After stirring at RT for 20 min, one aliquot of the solution was transferred to a different Schlenk flask and the solvent was removed by evaporation in vacuo. The solid residue was redissolved in THF-d₈ for NMR analysis.



¹H NMR (THF-d₈, 400 MHz): δ (ppm) = 6.95 (s, 1H, H^b), 6.93 (s, 2H, H^m), 6.65 (dd, *J* = 8.5, 1.5 Hz, 1H, H^c), 6.44 (dd, *J* = 7.0, 1.5 Hz, 1H, H^e), 6.39 (dd, *J* = 8.5, 7.0 Hz, 1H, H^d), 2.31 (s, 3H, CH₃^p), 1.95 (s, 6H, CH₃^o). ¹³C{¹H} NMR (THF-d₈, 101 MHz): δ (ppm) = 205.5 (N₂C), 161.2 (C-S), 141.0 (C_o-Mes), 137.7 (C_i-Mes), 136.0 (C_p-Mes), 134.8 (C_{im}Py), 129.4 (C-H^m Mes), 123.8 (C-H^d), 112.8 (C-H^e), 109.1 (C-H^b), 104.9 (C-H^c), 21.3 (CH₃^{para}), 18.0 (CH₃^{ortho}).

Preparation of 3

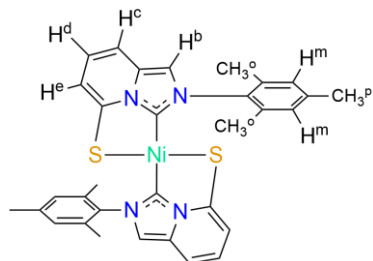


1-H (268 mg, 1.00 mmol) was weighed into a Schlenk flask and cycled 3 times before 20 mL dry THF were added under N₂ flow. 2.2 mL (1.10 mmol) of a 0.5 M solution of KHMDS in toluene were added dropwise to the yellow solution resulting in a color change to dark brown. After stirring at RT for 20 min the reaction mixture was cooled down to -35 °C before NiCl₂(dme) (121 mg, 0.55 mmol) was added as a solid to the reaction mixture under N₂ flow. The resulting dark green reaction mixture was slowly warmed to RT and stirred overnight. The solvents were removed by evaporation in vacuo and the green residue was redissolved

Supporting Information

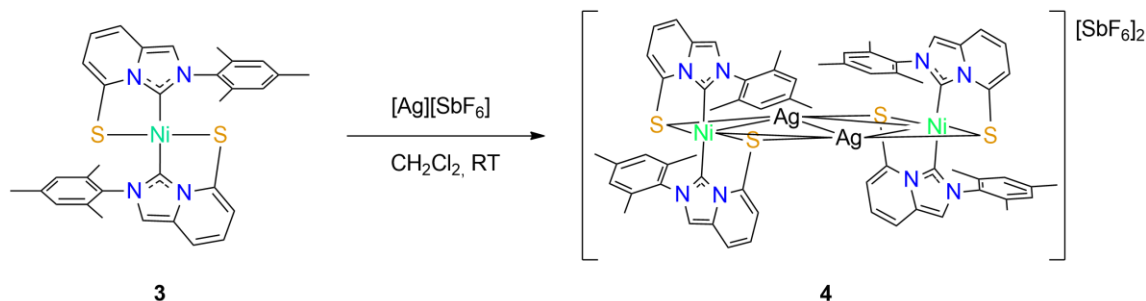
in CH₂Cl₂ and filtered through a Celite plug to remove salts that formed during the reaction. The Celite plug was washed with CH₂Cl₂ until the filtrate became colorless. The solvent of the filtrate was removed under reduced pressure and the residue was purified by column chromatography (silica gel, 100 % CH₂Cl₂) to obtain 163 mg (0.27 mmol, 55 %) of the title compound as a red solid. Single crystals suitable for X-ray diffraction analysis were obtained by vapor diffusion of diethylether into a concentrated solution of the product in CH₂Cl₂.

¹H NMR (CDCl₃, 400 MHz): δ (ppm) = 7.06 (s, 4H, H^m), 6.89 (d, *J* = 8.9 Hz, 2H, H^c), 6.89 (s, 2H, H^b), 6.80 (dd, *J* = 8.9, 6.9 Hz, 2H, H^d), 6.53 (d, *J* = 6.9 Hz, 2H, H^e), 2.45 (s, 6H, CH₃ para), 2.07 (s, 12H, CH₃ ortho). ¹³C{¹H} NMR (CDCl₃, 101 MHz): δ (ppm) = 159.3 (N₂C), 150.1 (C-S), 139.5 (C_{Mes-p}), 136.6 (C_{Mes-i}), 135.6 (C_{Mes-o}), 130.8 (C_{imPy}), 129.2 (C-H^m), 124.9 (C-H^d), 112.1 (C-H^b), 108.8 (C-H^e), 107.5 (C-H^c), 21.5 (CH₃ para), 18.0 (CH₃ ortho). MALDI-TOF MS: *m/z*: calc. for C₃₂H₃₀N₄NiS₂: 592.1; found: 592.2. Elemental analysis: calc. for C₃₂H₃₀N₄NiS₂: C 64.77 %, H 5.10 %, N 9.44 %; found: C 64.26 %, H 5.10 %, N 9.58 %.



Preparation of 4

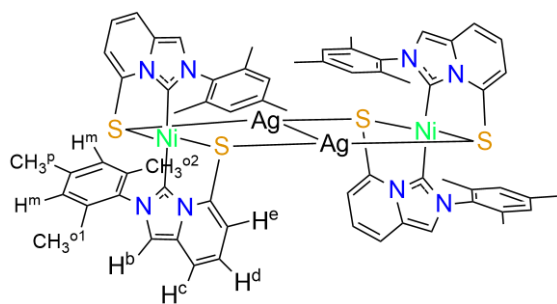
3 (30 mg, 0.051 mmol) was weighed into a Schlenk flask and cycled 3 times before 2 mL of



dry CH₂Cl₂ were added. Ag[SbF₆] (21 mg, 0.061 mmol) was added under N₂ flow to the greenish red solution resulting in an immediate color change to olive-green. After stirring at RT for 30 min the green solution was filtered through a Celite pad which was then washed with more CH₂Cl₂. The solvent of the filtrate was removed by evaporation in vacuo to obtain the title compound as an olive-green solid (12 mg, 0.006 mmol, 26 %). Single crystals suitable for X ray diffraction analysis were obtained by layering diethylether on a concentrated solution of the product in 1,2-dichloroethane.

¹H NMR (CD₂Cl₂, 300 MHz): δ (ppm) = 7.41 (d, *J* = 9.0 Hz, 4H H^c), 7.37 (s, 4H, H^b), 7.11 (dd, *J* = 9.0, 7.0 Hz, 4H, H^d), 7.05 (s, 8H, H^m), 6.79 (d, *J* = 7.0 Hz, 4H, H^e), 2.47 (s, 12H, CH₃ para), 1.90 (s, 12H, CH₃ ortho), 1.64 (s, 12H, CH₃ ortho).

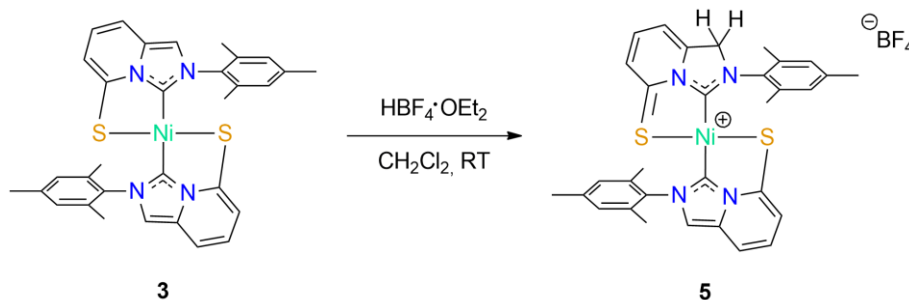
Supporting Information



$^{13}\text{C}\{^1\text{H}\}$ NMR (CD_2Cl_2 , 101 MHz): δ (ppm) = 152.2 (N_2C), 142.1 ($\text{C}_{p\text{-Mes}}$), 135.4 (C-S), 134.7 ($\text{C}_{i\text{-Mes}}$), 133.2 ($\text{C}_{o\text{-Mes}}$), 131.8 (C_{ImPy}), 131.1 (C-H^m), 130.0 (C-H^m), 126.1 (C-H^d), 117.6 (C-H^b), 115.66, 115.64 (C-H^c , C-H^e), 21.5 (CH_3 para), 18.2 (CH_3 ortho), 17.9 (CH_3 ortho).

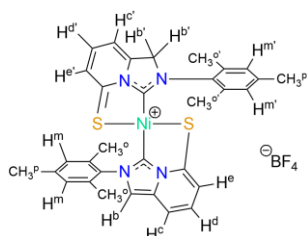
^{19}F NMR (CD_3CN , 376 MHz): δ (ppm) = -111.1 - -136.9 (m, SbF_6^- , 1J coupling of ^{19}F with ^{121}Sb ($I = 5/2$) and with ^{123}Sb ($I = 7/2$)). MALDI-TOF MS: m/z : calc. for $\text{C}_{64}\text{H}_{61}\text{Ag}_2\text{N}_8\text{Ni}_2\text{S}_4$: 1403.1; found: 1404.0; calc. for $\text{C}_{64}\text{H}_{61}\text{AgN}_8\text{Ni}_2\text{S}_4$: 1294.2; found: 1294.5. Elemental analysis: calc. for $\text{C}_{64}\text{H}_{60}\text{Ag}_2\text{F}_{12}\text{N}_8\text{Ni}_2\text{S}_4\text{Sb}_2 + 2 \text{CH}_2\text{Cl}_2$: C 38.78 %, H 3.16 %, N 5.48 %; found: C 38.51 %, H 3.02 %, N 5.60 %.

Preparation of **5**



3 (40 mg, 0.067 mmol) was weighed into a Schlenk flask and cycled 3 times before 2 mL of dry CH_2Cl_2 were added. 10 μL of $\text{HBF}_4 \cdot \text{OEt}_2$ (0.074 mmol) was added dropwise via microsyringe under N_2 flow to the greenish red solution resulting in a color change to dark green. After stirring at RT for 1 h the solvent was removed in vacuo to obtain a dark green solid.

^1H NMR (CDCl_3 , 400 MHz): δ (ppm) = 7.87 (dd, $J = 8.7, 7.2$ Hz, 1H, H^d), 7.69 (d, $J = 7.2$ Hz, 1H, H^c), 7.43 (d, $J = 8.7$ Hz, 1H, H^e), 7.23 (s, 1H, H^b), 7.22 (dd, $J = 9.0, 0.8$ Hz, 1H, H^c),



7.11 (s, 2H, H^m/H^m) 7.10 (s, 2H, H^m/H^m), 7.09 (dd, $J = 9.0, 7.1$ Hz, H^d), 6.83 (dd, $J = 7.1, 0.8$ Hz, 1H, H^e), 5.43 (s, 2H, H^b), 2.48 (s, 3H, CH_3 para), 2.45 (s, 3H, CH_3 para), 2.29 (s, 6H, CH_3 ortho), 2.00 (s, 6H, CH_3 ortho). $^{13}\text{C}\{^1\text{H}\}$ NMR (CDCl_3 , 101 MHz): δ (ppm) = 206.0 ($\text{N}_2\text{C}'$), 172.8 ($\text{C-S}'$), 152.8 (N_2C), 146.6 (C_{ImPy}), 146.3 (C-S),

143.1 (C-H^d), 141.6 ($\text{C}_{p\text{-Mes}}$), 140.8 ($\text{C}_{p\text{-Mes}}$), 139.5 ($\text{C}_{i\text{-Mes}}$), 135.5 ($\text{C}_{o\text{-Mes}}$), 133.8 ($\text{C}_{o\text{-Mes}}$), 133.2 ($\text{C}_{i\text{-Mes}}$), 130.8-130.7 (CH^m/m'), 129.6-129.2 (CH^m/m'), 126.2 (C-H^e), 125.6 (C-H^d), 114.6 (C-H^b), 113.2 (C-H^c), 111.6 (C-H^e), 109.7 (C-H^c), 65.4 (CH_2^b), 21.51-21.48 (CH_3 para), 18.1-18.0-17.7 (CH_3 ortho). ^{19}F NMR (CDCl_3 , 376 MHz): δ (ppm) = -152.53/-152.58 (1:3, BF_4^-).

Supporting Information

Chemical oxidation experiments of complex **3**

3 easily reacted with various organic and inorganic oxidizing agents such as $\text{Fc}(\text{BF}_4)$, $(\text{NO})(\text{SbF}_6)$, PhICl_2 or CuCl_2 but the nature of the products could not be firmly determined in most of cases. The reaction of **3** with CuCl_2 was shown to give the cleanest reaction outcome and is described hereafter: The reaction of **3** with anhydrous CuCl_2 in dichloromethane and subsequent MALDI-MS analysis of the crude product mixture allowed the identification of three formally Ni(III) complexes with the following composition: $\text{Ni}[\mathbf{1}]_3$ (**6**), $\text{NiCl}[\mathbf{1}]_2$ (**7**), and $\text{NiCl}[\mathbf{1}]_3$ (**8**) (Scheme S1). These were assigned based on the peaks detected at m/z 860.35, 628.49, and 894.12 (in order of intensity), corresponding to the cations $[\mathbf{6}+\text{H}^+]$, $[\mathbf{7}+\text{H}^+]$, and $[\mathbf{8}]^+$, respectively (Figure S1). The structure of **8** is tentatively assigned as containing a dimerized neutral version of **1** through a disulfide bridge. Interestingly, when the reaction was carried out under “wet” conditions with $\text{CuCl}_2 \cdot 2\text{H}_2\text{O}$ in degassed dichloromethane, ESI-MS analysis was consistent with the formation of **6** almost exclusively (Figure S2). Unfortunately, although the MS spectrum of the compound purified by flash chromatography was identical, we were unable to firmly confirm the structure by other spectroscopic or analytical techniques.

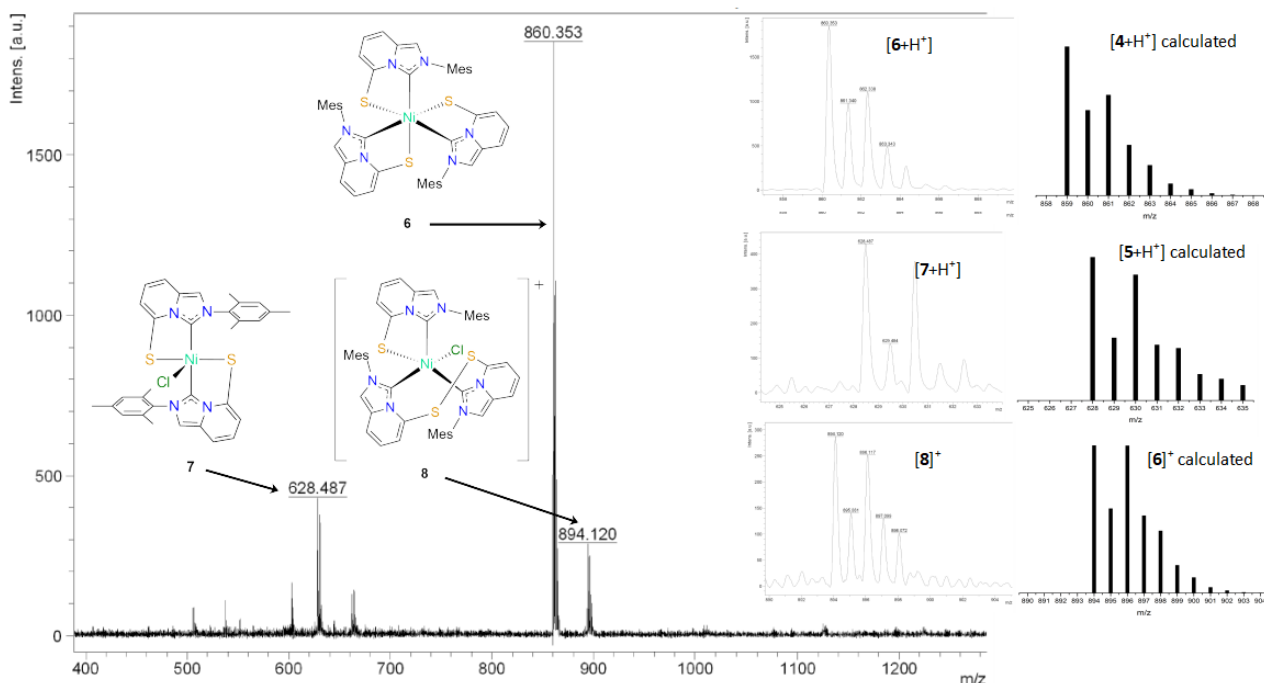


Figure S1. MALDI-MS spectrum of the crude product obtained by reaction of **3** with anhydrous CuCl_2 .

Supporting Information

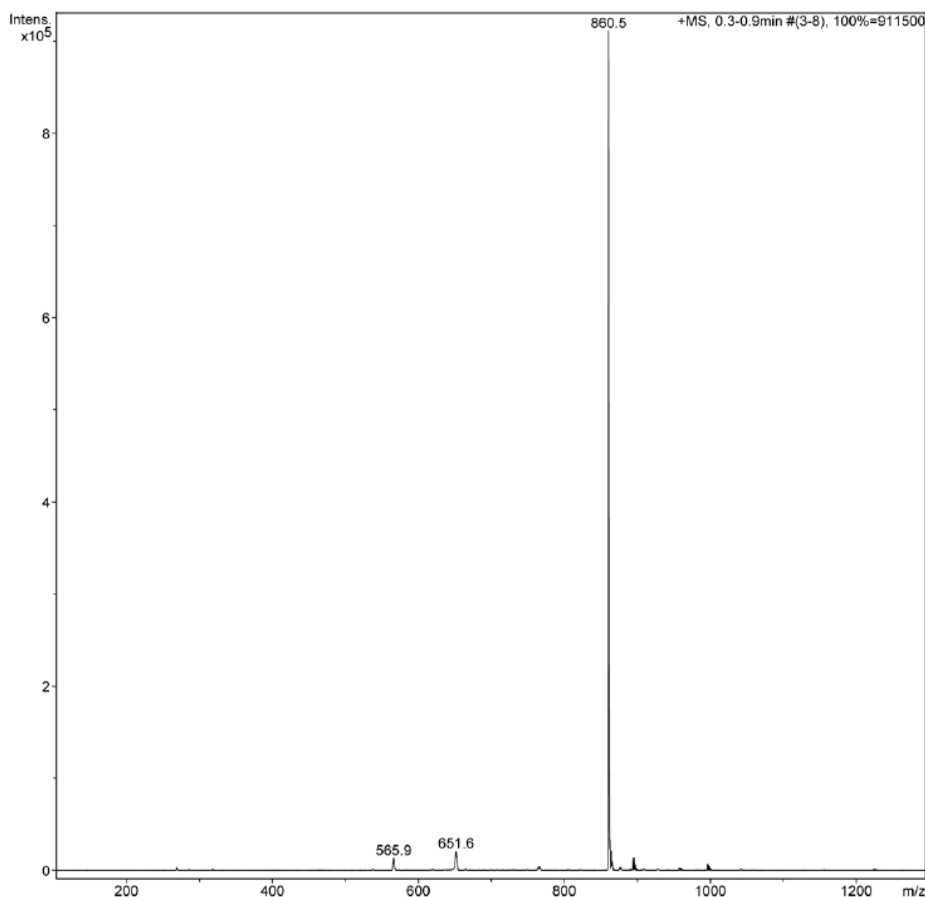


Figure S2. ESI ion trap mass spectrum of the crude product obtained from the reaction of **3** with $\text{CuCl}_2 \cdot 2\text{H}_2\text{O}$.

X-Ray analysis

Data were collected at low temperature (100 K) on a XtaLAB Synergy diffractometer using a Cu-K α radiation ($\lambda = 1.54184 \text{ \AA}$) micro-source, equipped with an Oxford Cryosystems Cooler Device. The structures have been solved using the new dual-space algorithm program SHELXT,⁵ and refined by means of least-squares procedures using either SHELXL-2018¹ program included in the software package WinGX⁶ version 1.639, or with the aid of the program CRYSTALS.⁷ The Atomic Scattering Factors were taken from International Tables for X-Ray Crystallography.⁸ Hydrogen atoms were placed geometrically and refined using a riding model. All non-hydrogen atoms were anisotropically refined.

Ellipsoid plots in the figures of the crystallography section were generated using the software ORTEP-35.⁹ The crystal structures have been deposited at the Cambridge Crystallographic Data Centre and allocated the deposition numbers CCDC 2449873-2449875.

Supporting Information

NMR Spectra

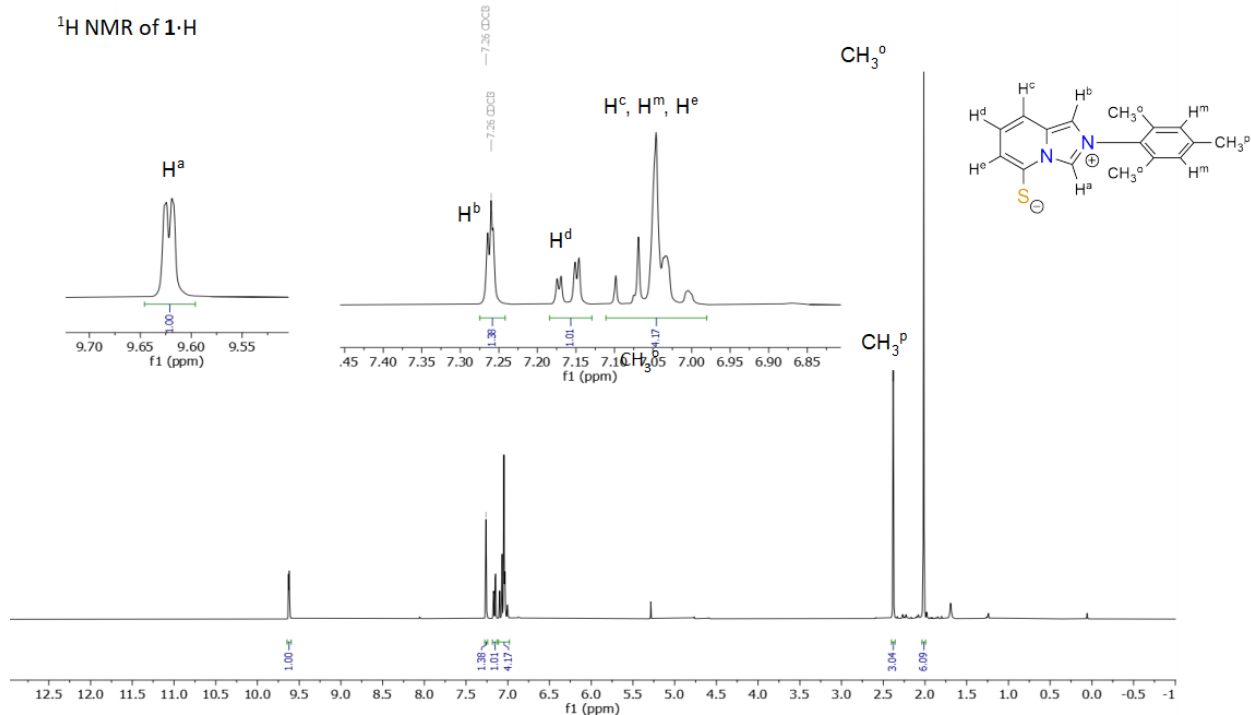


Figure S3. ^1H NMR spectrum of $1\cdot\text{H}$ (CDCl_3 , 300 MHz).

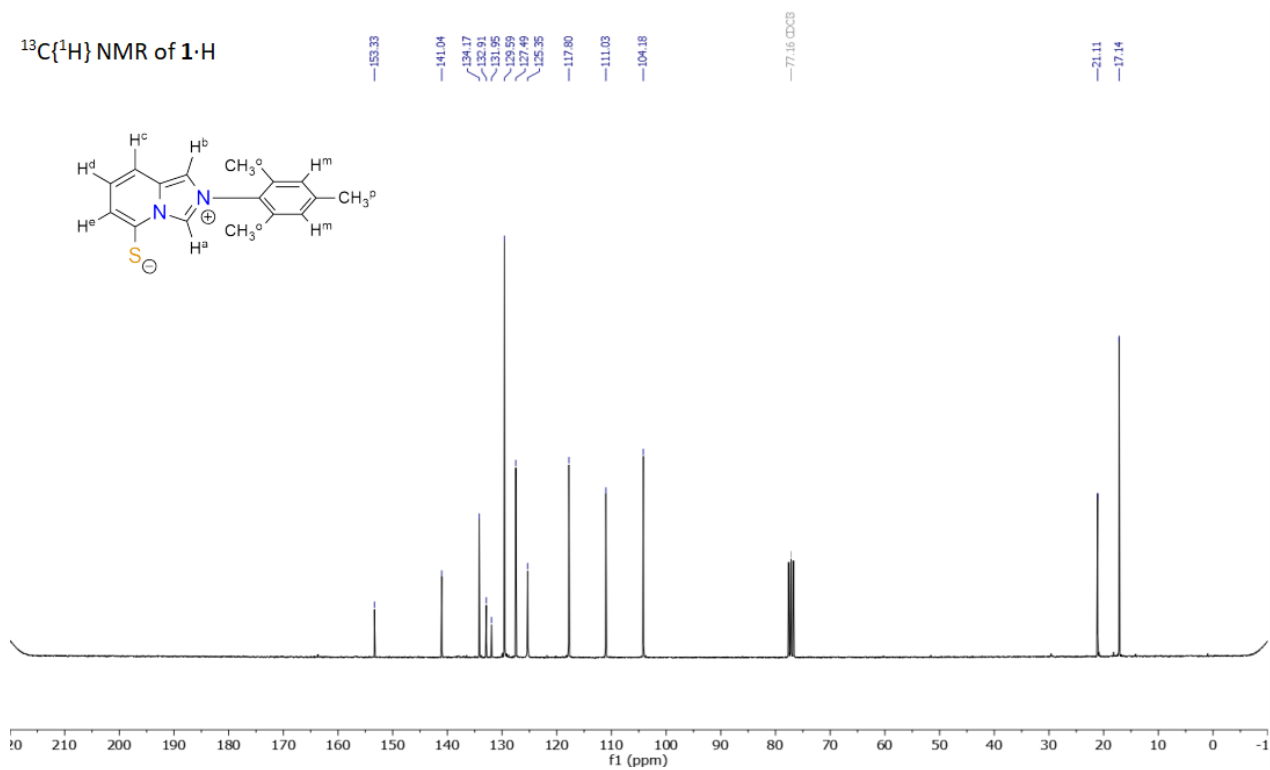


Figure S4. $^{13}\text{C}\{^1\text{H}\}$ NMR spectrum of $1\cdot\text{H}$ (CDCl_3 , 75 MHz).

Supporting Information

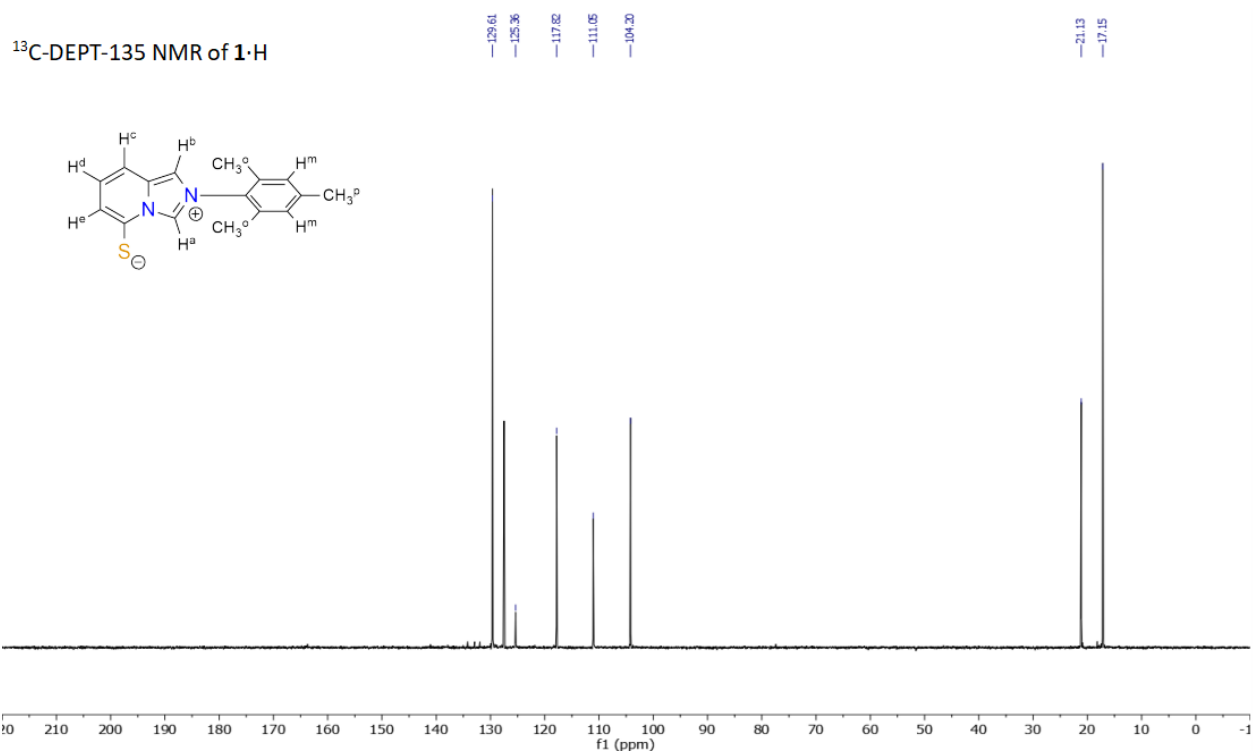


Figure S5. ^{13}C DEPT 135 NMR spectrum of **1**·H (CDCl_3 , 75 MHz).

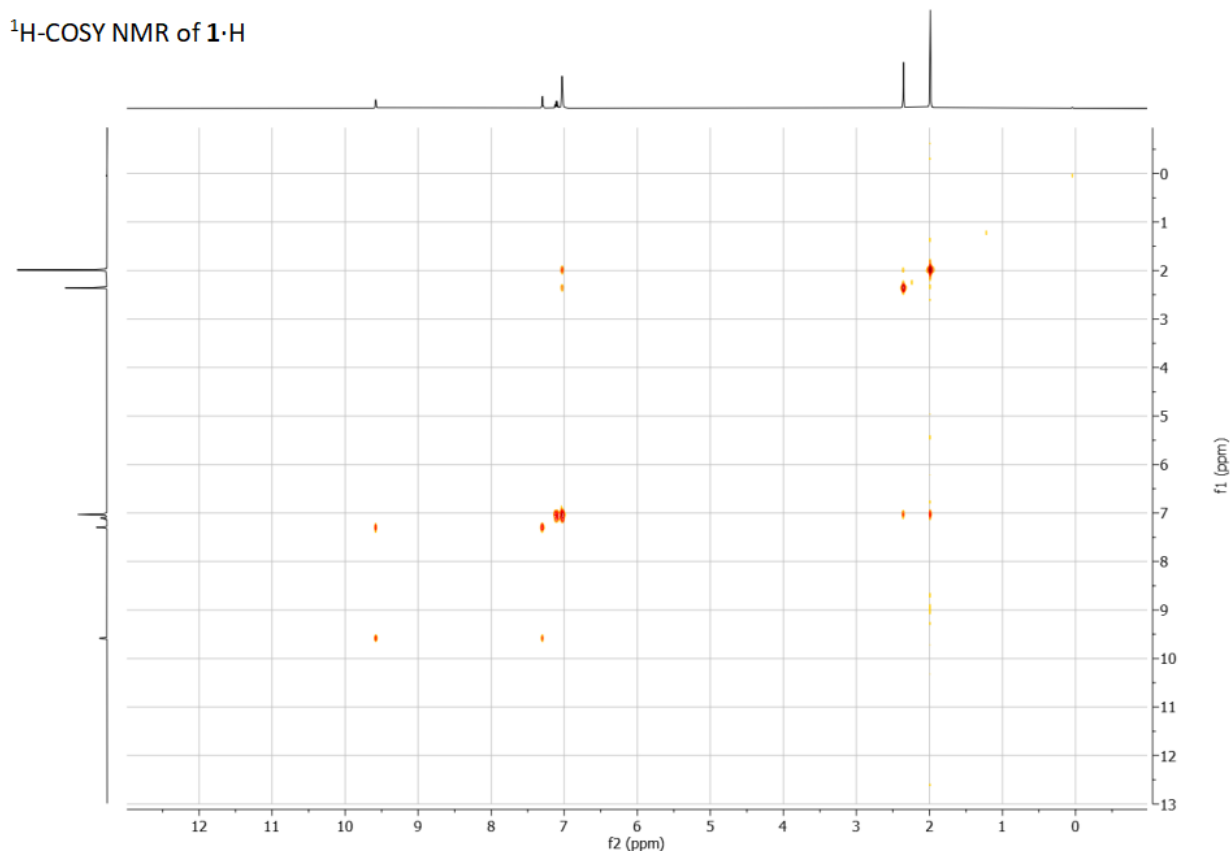


Figure S6. ^1H - ^1H COSY NMR spectrum of **1**·H (CDCl_3 , 300 / 300 MHz).

Supporting Information

^1H - ^{13}C -HSQC NMR of **1**-H

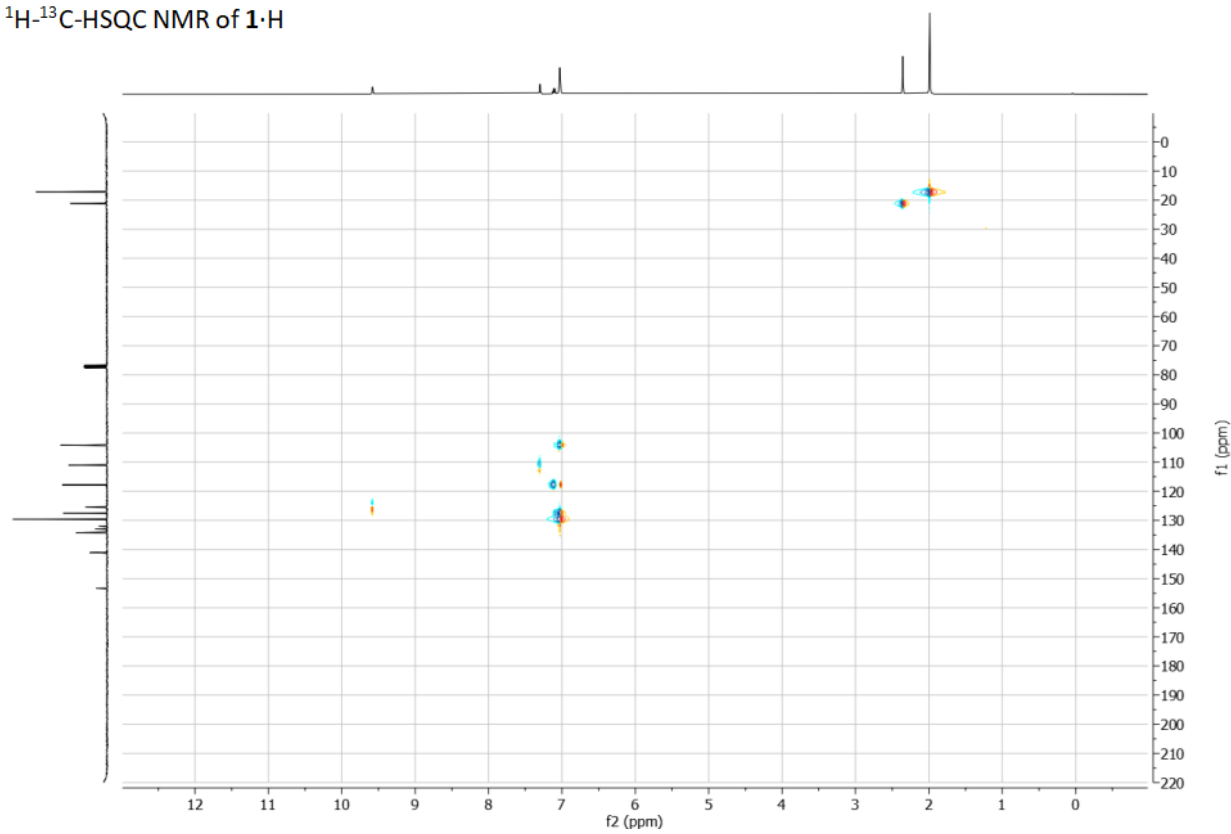


Figure S7. ^1H - ^{13}C HSQC NMR spectrum of **1**-H (CDCl_3 , 300 / 75 MHz).

Supporting Information

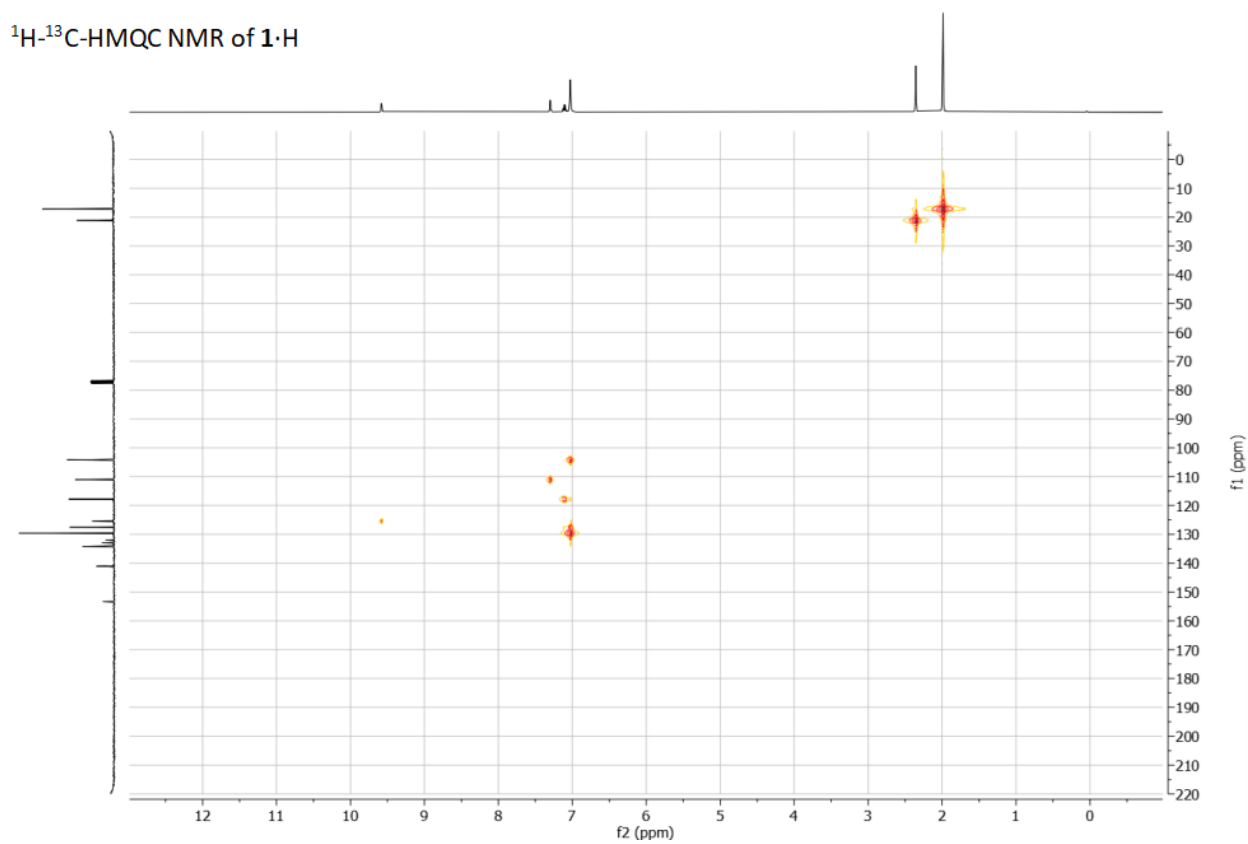
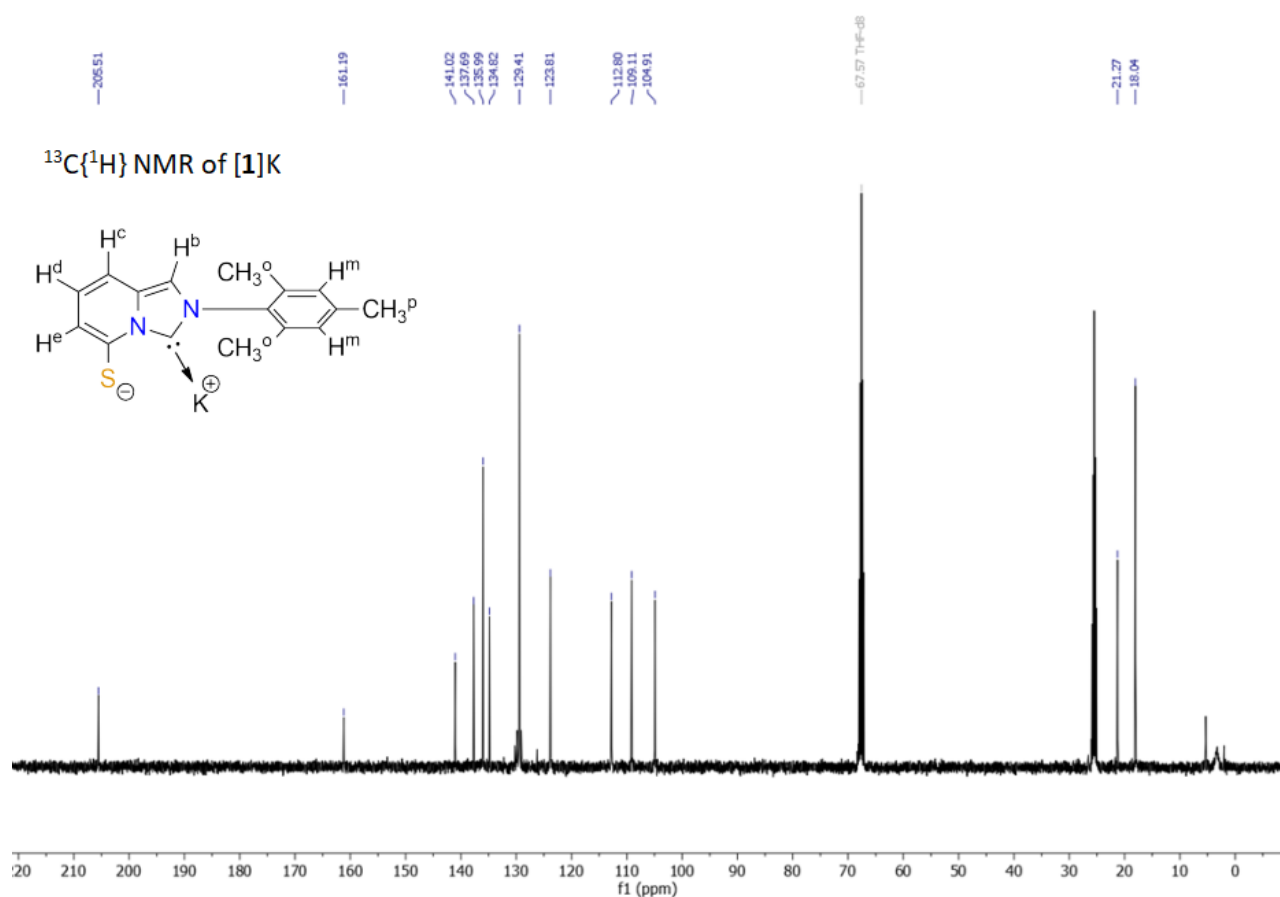
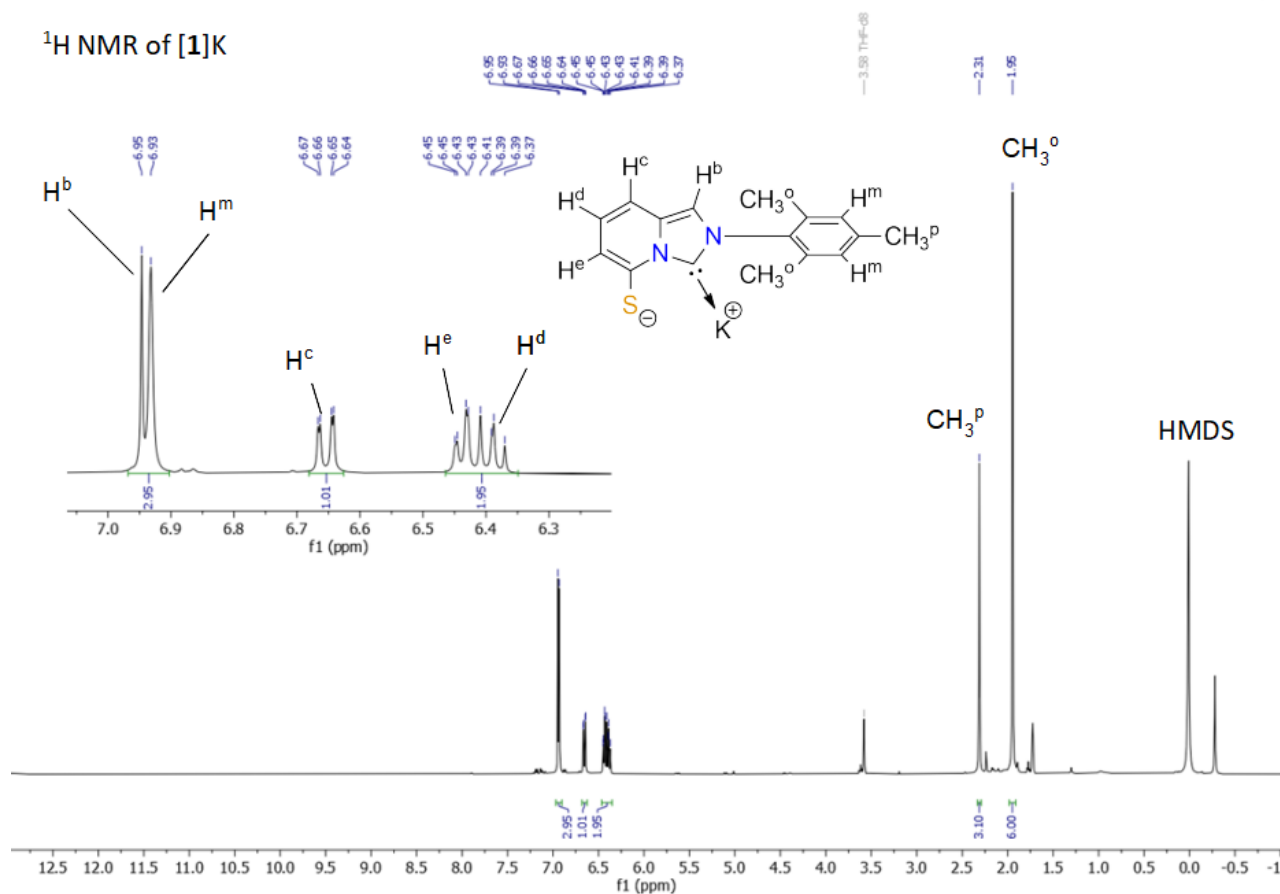


Figure S8. ^1H - ^{13}C HMQC NMR spectrum of **1**·H (CDCl_3 , 300 / 75 MHz).

Supporting Information



Supporting Information

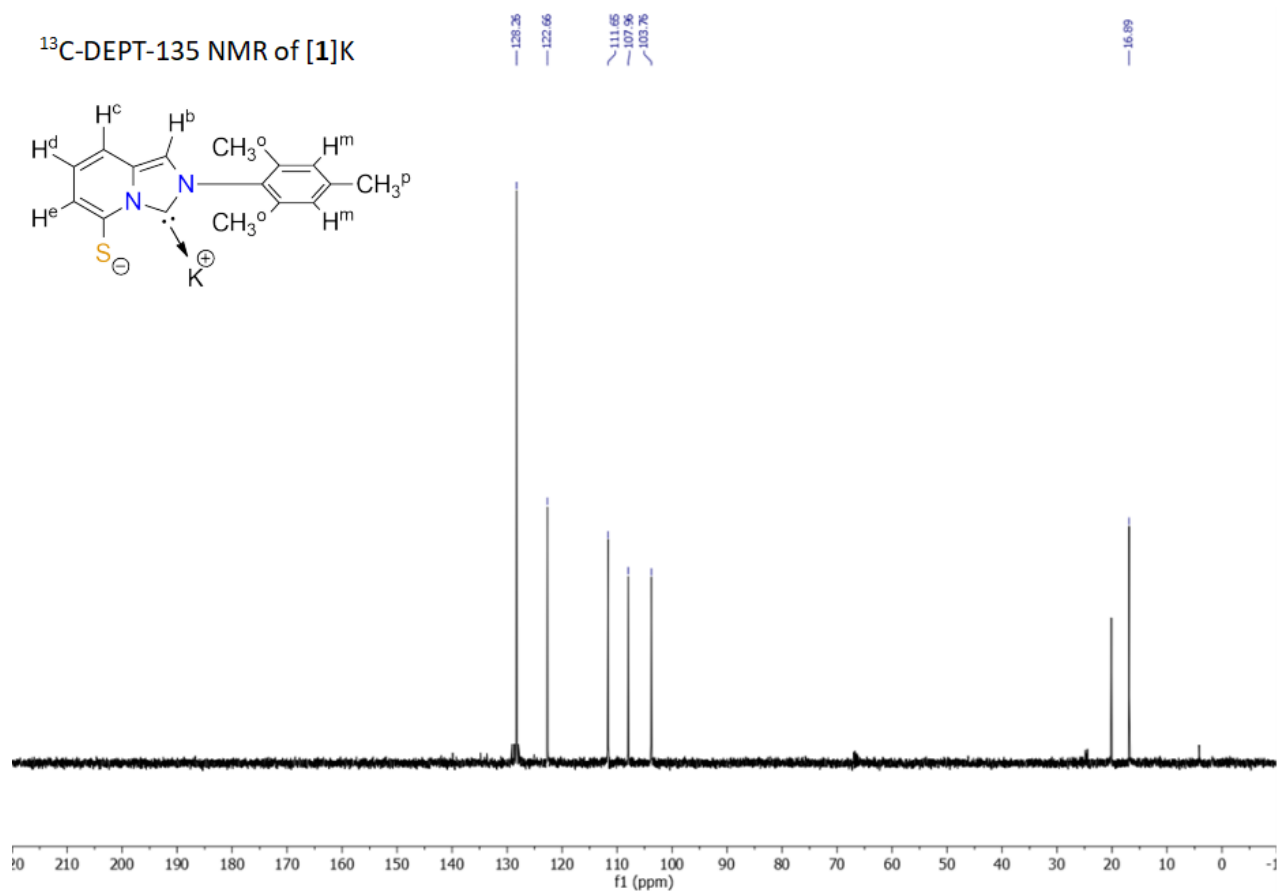


Figure S11. ^{13}C DEPT 135 NMR spectrum of [1]K (THF- d_8 , 101 MHz).

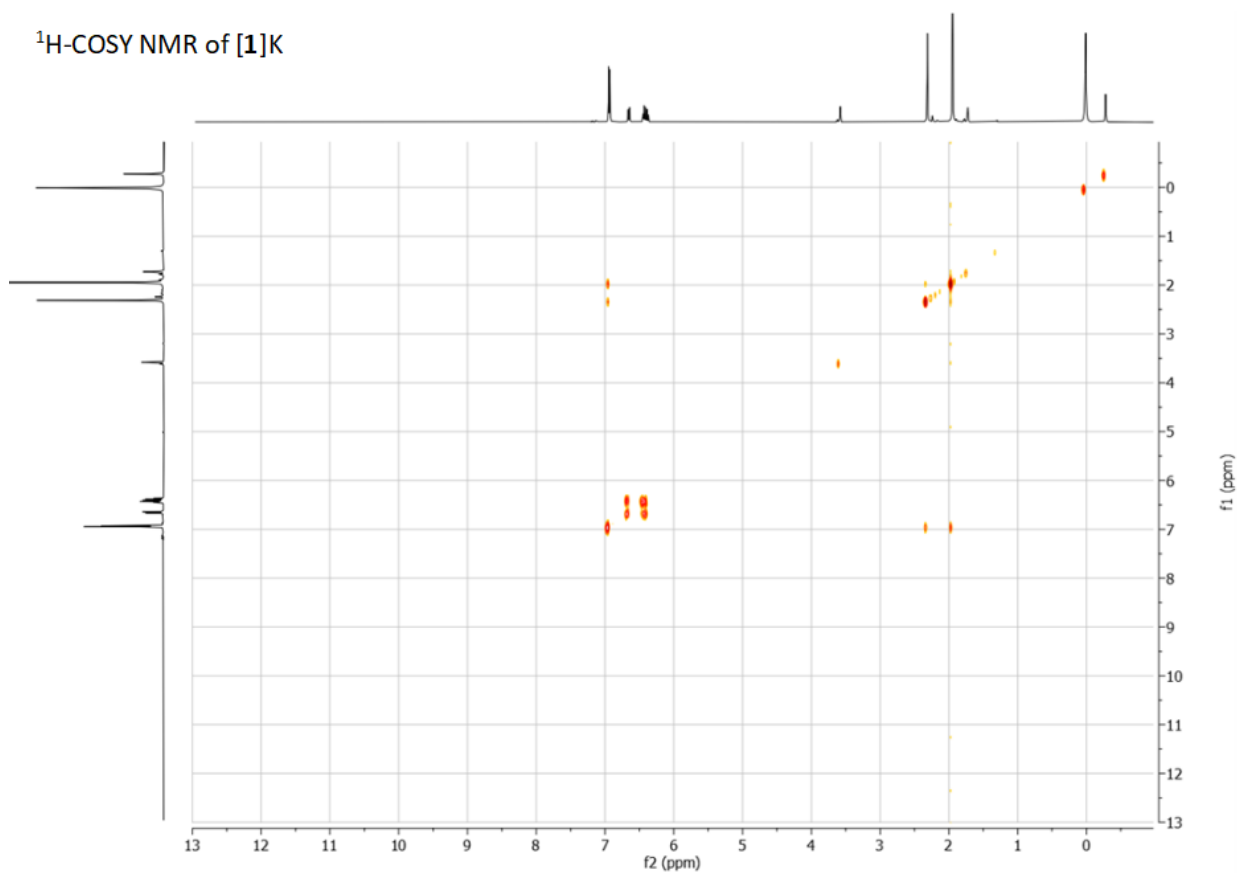


Figure S12. ^1H - ^1H COSY NMR spectrum of [1]K (THF- d_8 , 400 / 400 MHz).

Supporting Information

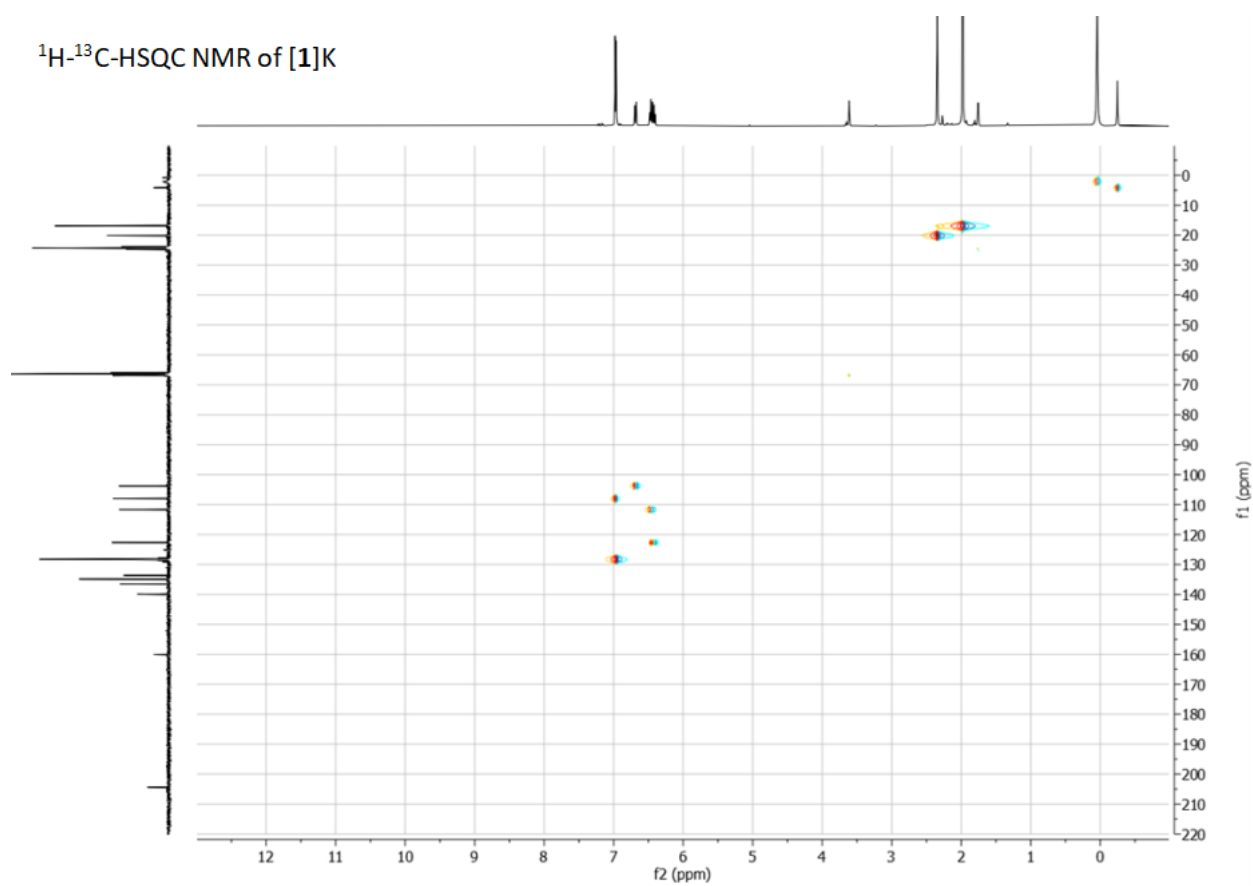


Figure S13. ^1H - ^{13}C HSQC NMR spectrum of [1]K (THF- d_8 , 400 / 101 MHz).

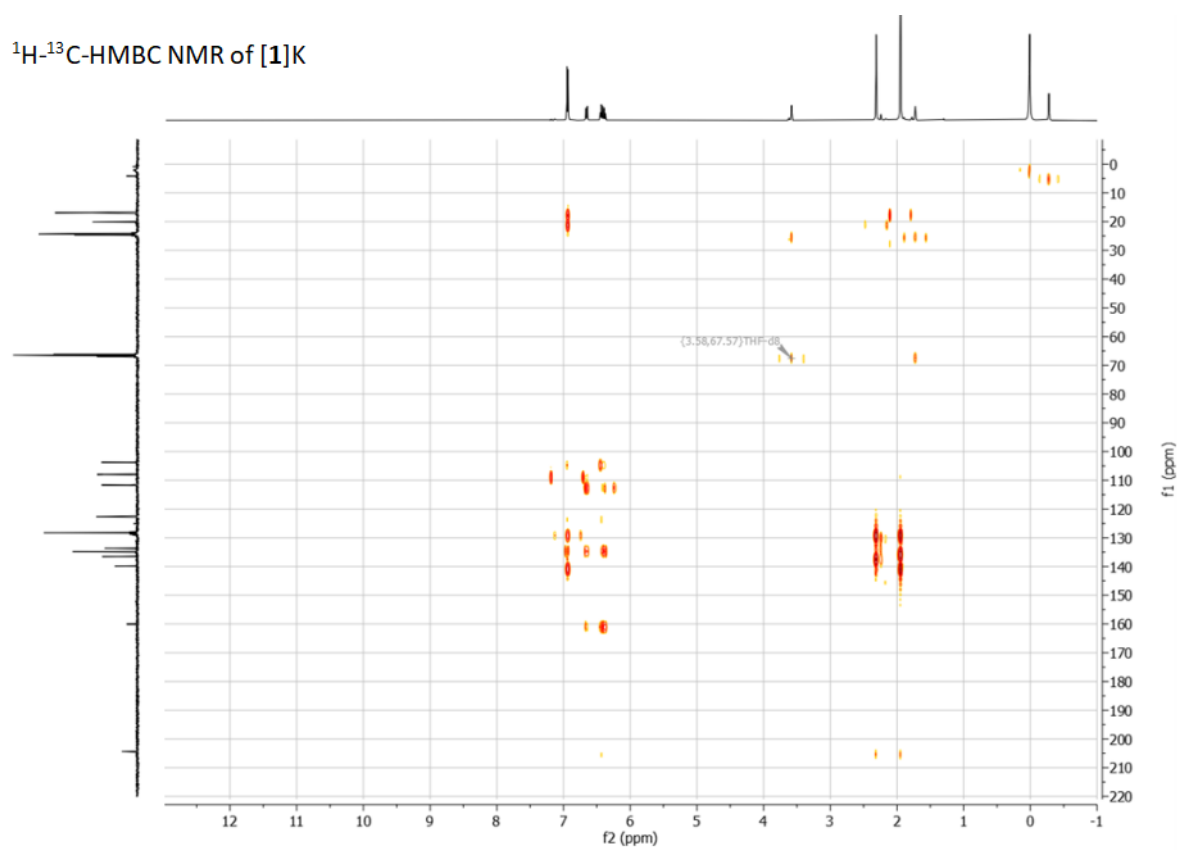


Figure S14. ^1H - ^{13}C HMBC NMR spectrum of [1]K (THF- d_8 , 400 / 101 MHz).

Supporting Information

^1H NMR of **3**

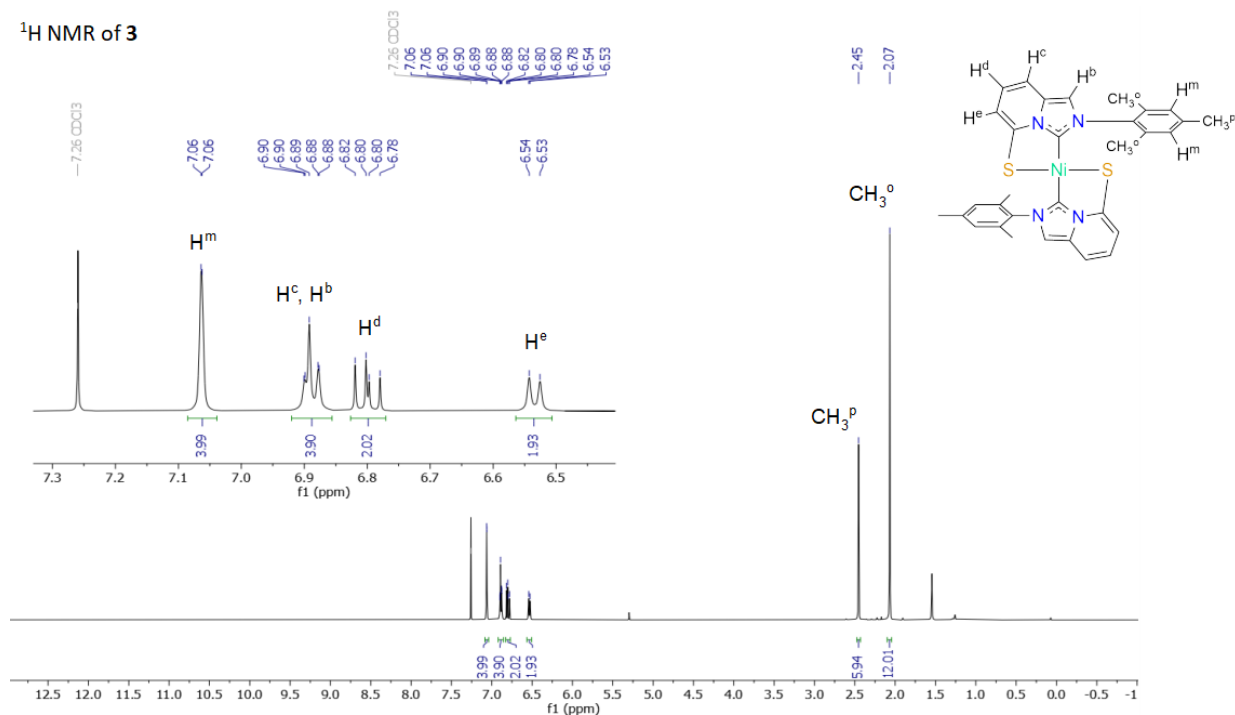


Figure S15. ^1H NMR spectrum of **3** (CDCl₃, 400 MHz).

$^{13}\text{C}\{^1\text{H}\}$ NMR of **3**

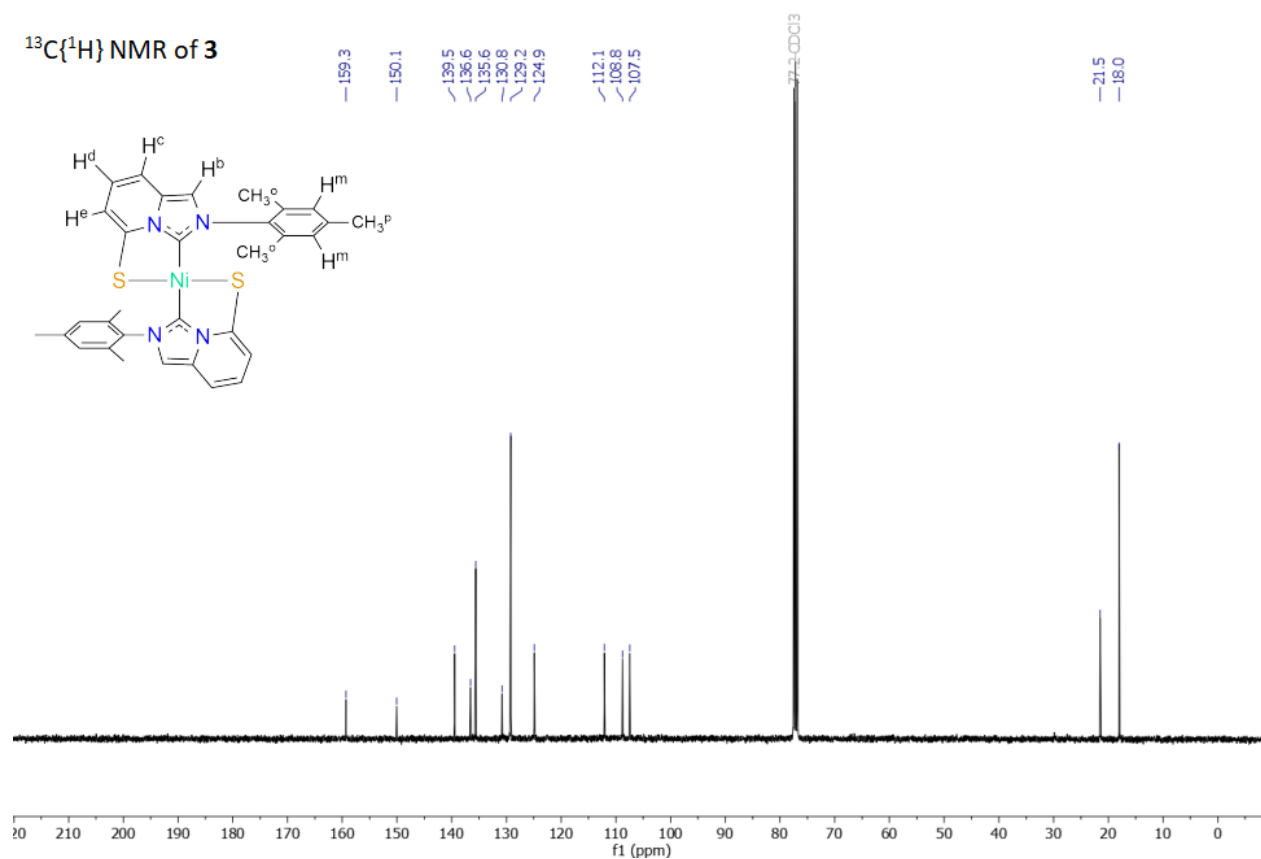


Figure S16. $^{13}\text{C}\{^1\text{H}\}$ NMR spectrum of **3** (CDCl₃, 101 MHz).

Supporting Information

^{13}C -DEPT-135 NMR of **3**

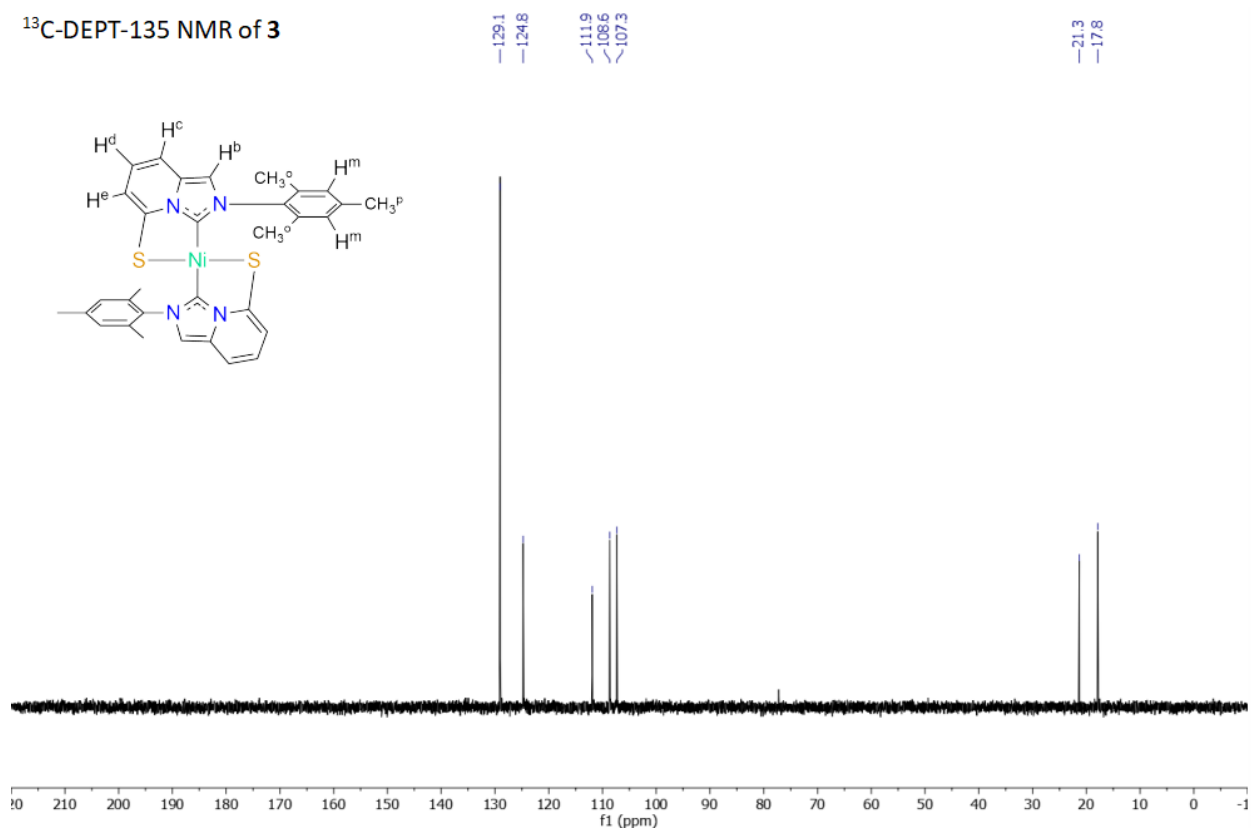


Figure S17. ^{13}C DEPT 135 NMR spectrum of **3** (CDCl₃, 101 MHz).

^1H -COSY NMR of **3**

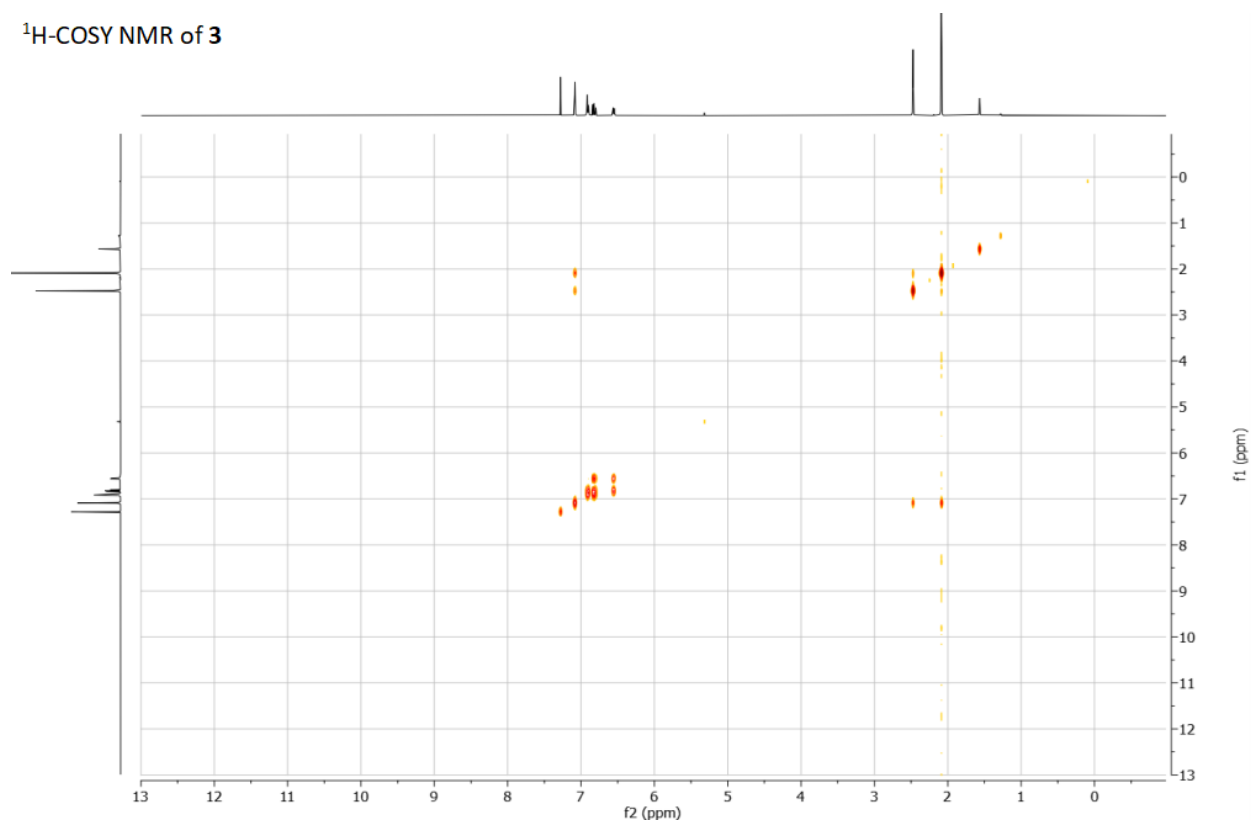


Figure S18. ^1H - ^1H COSY NMR spectrum of **3** (CDCl₃, 400 / 400 MHz).

Supporting Information

^1H - ^{13}C -HSQC NMR of **3**

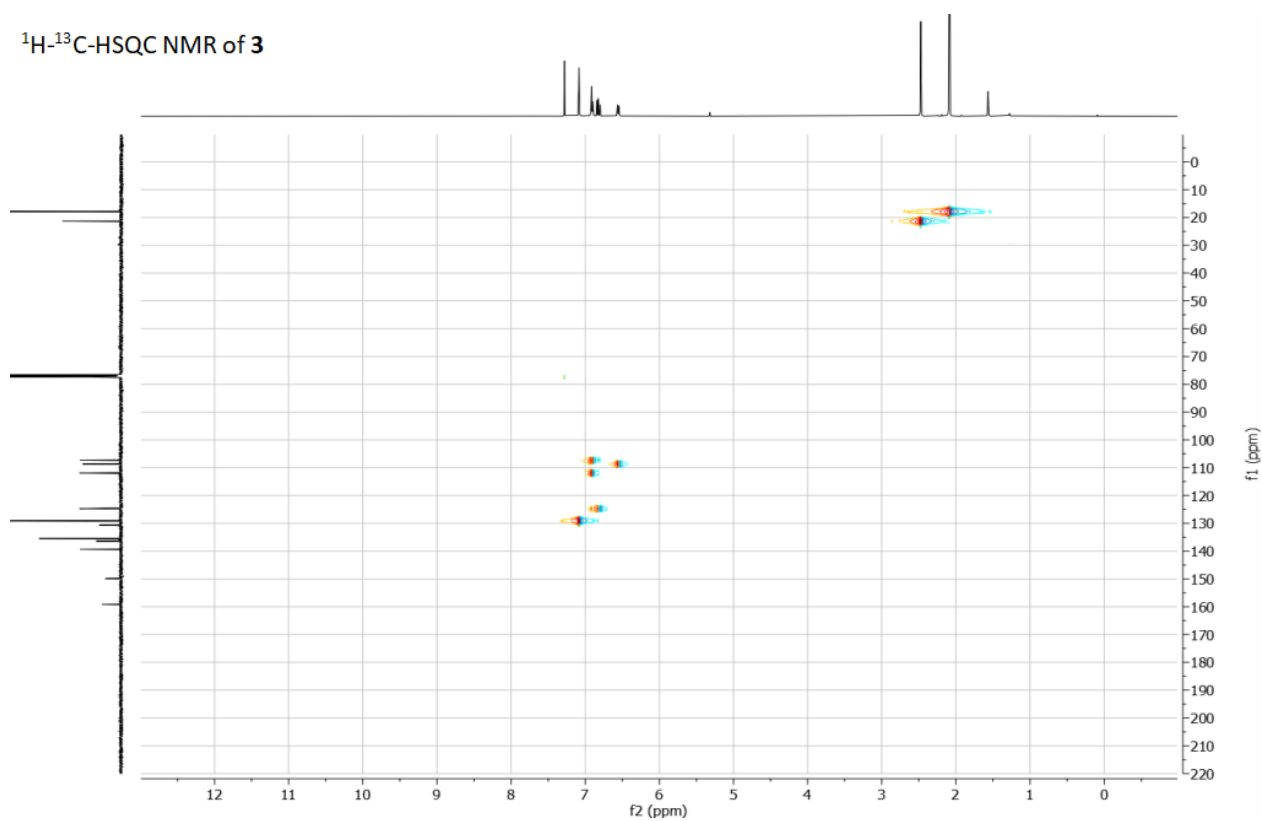


Figure S19. ^1H - ^{13}C HSQC NMR spectrum of **3** (CDCl_3 , 400 / 101 MHz).

^1H - ^{13}C -HMBC NMR of **3**

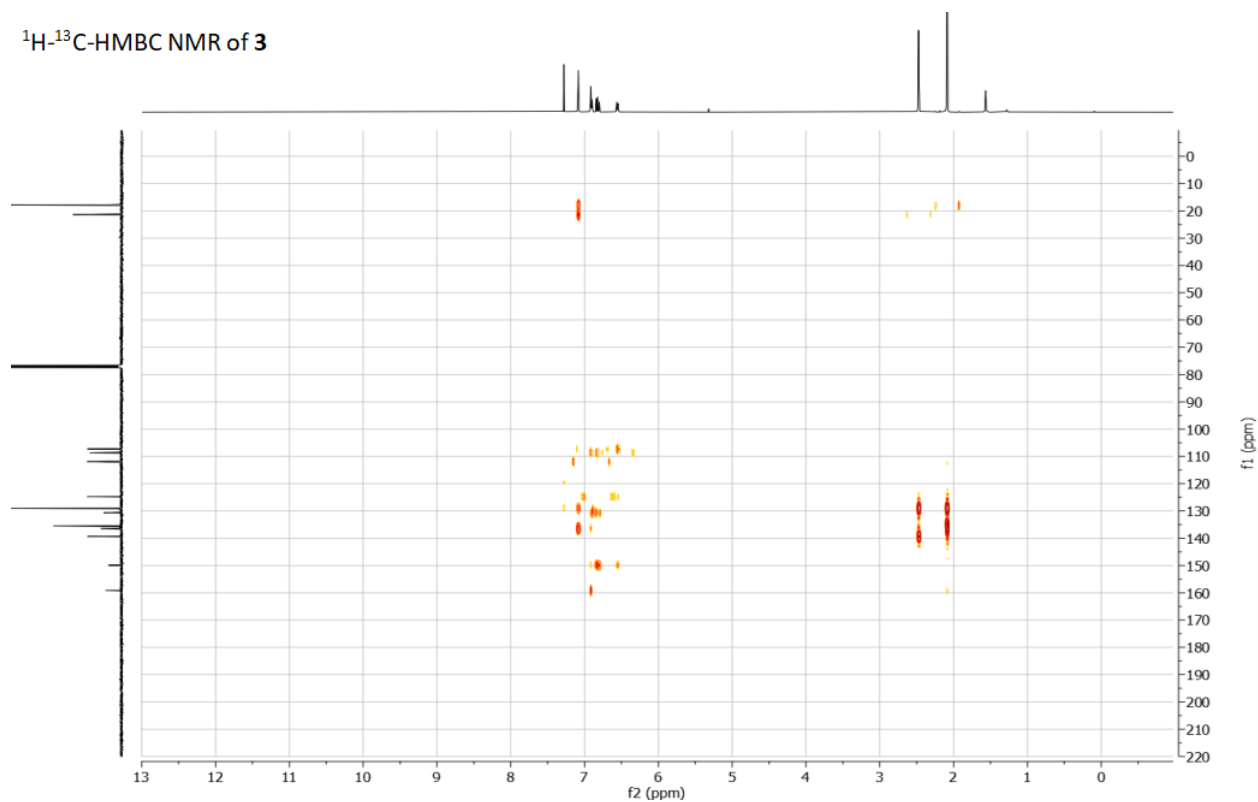


Figure S20. ^1H - ^{13}C HMBC NMR spectrum of **3** (CDCl_3 , 400 / 101 MHz).

Supporting Information

^1H NMR of **4**

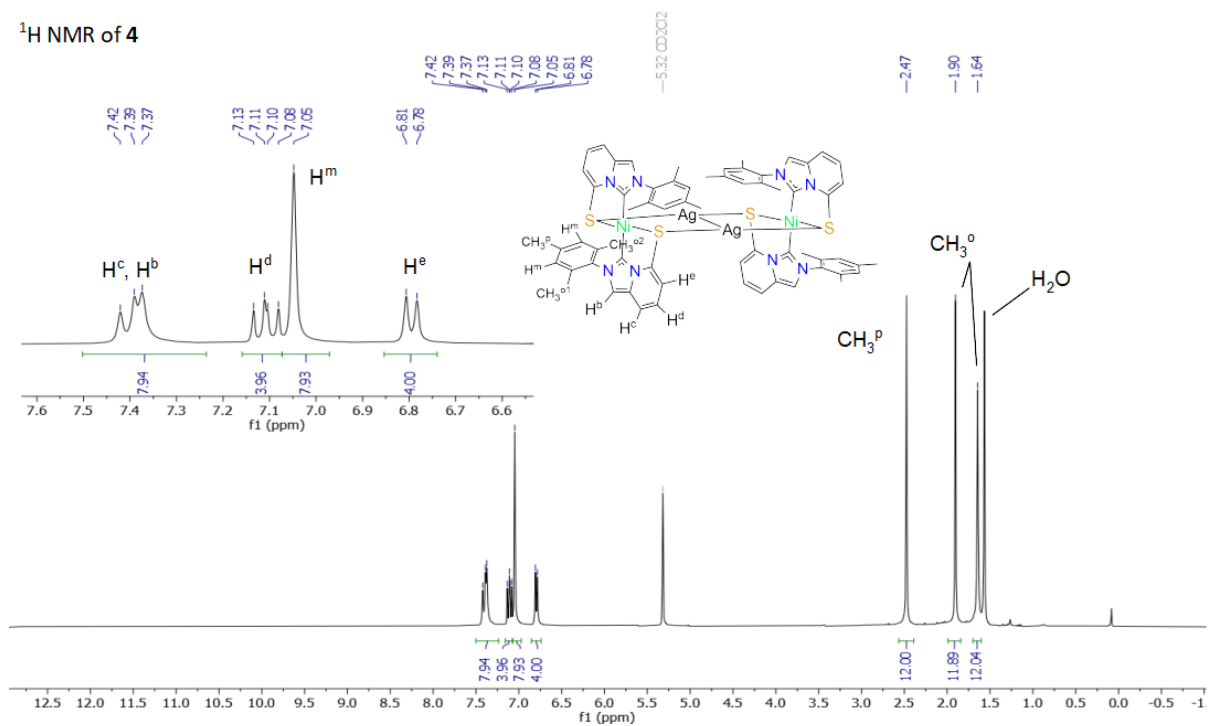


Figure S21. ^1H NMR spectrum of **4** (CD_2Cl_2 , 300 MHz).

$^{13}\text{C}\{^1\text{H}\}$ NMR of **4**

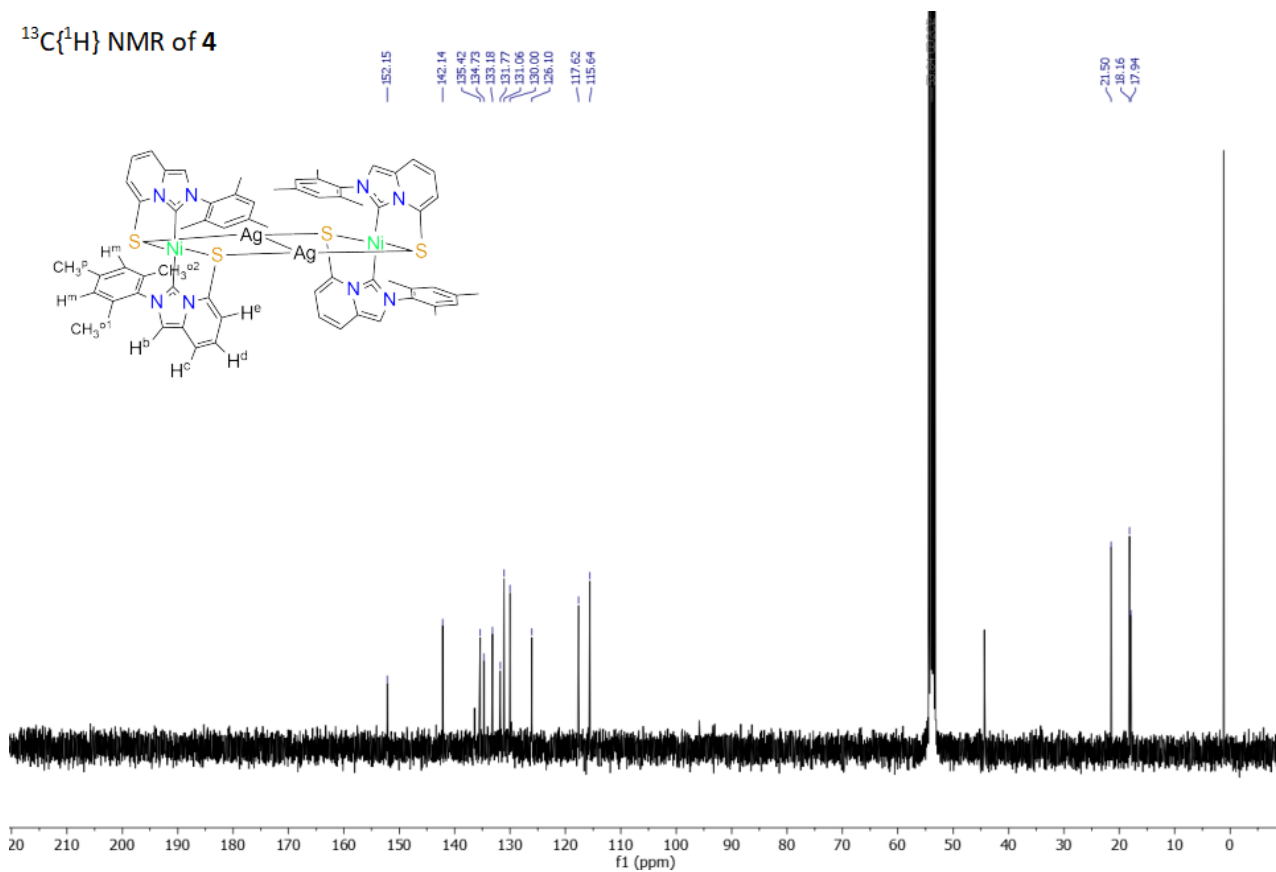


Figure S22. $^{13}\text{C}\{^1\text{H}\}$ NMR spectrum of **4** (CD_2Cl_2 , 101 MHz).

Supporting Information

^{13}C -DEPT-135 NMR of **4**

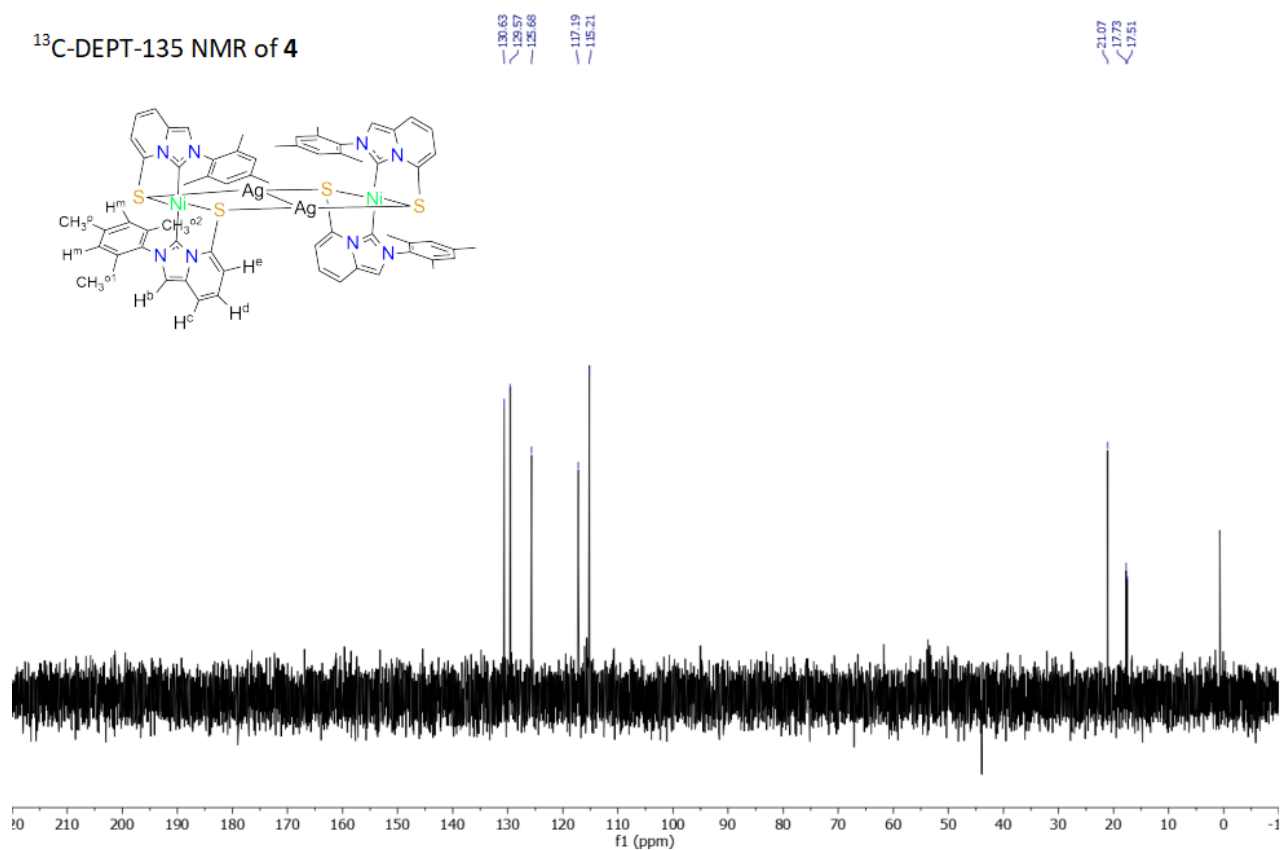


Figure S23. ^{13}C DEPT 135 NMR spectrum of **4** (CD_2Cl_2 , 101 MHz).

^1H -COSY NMR of **4**

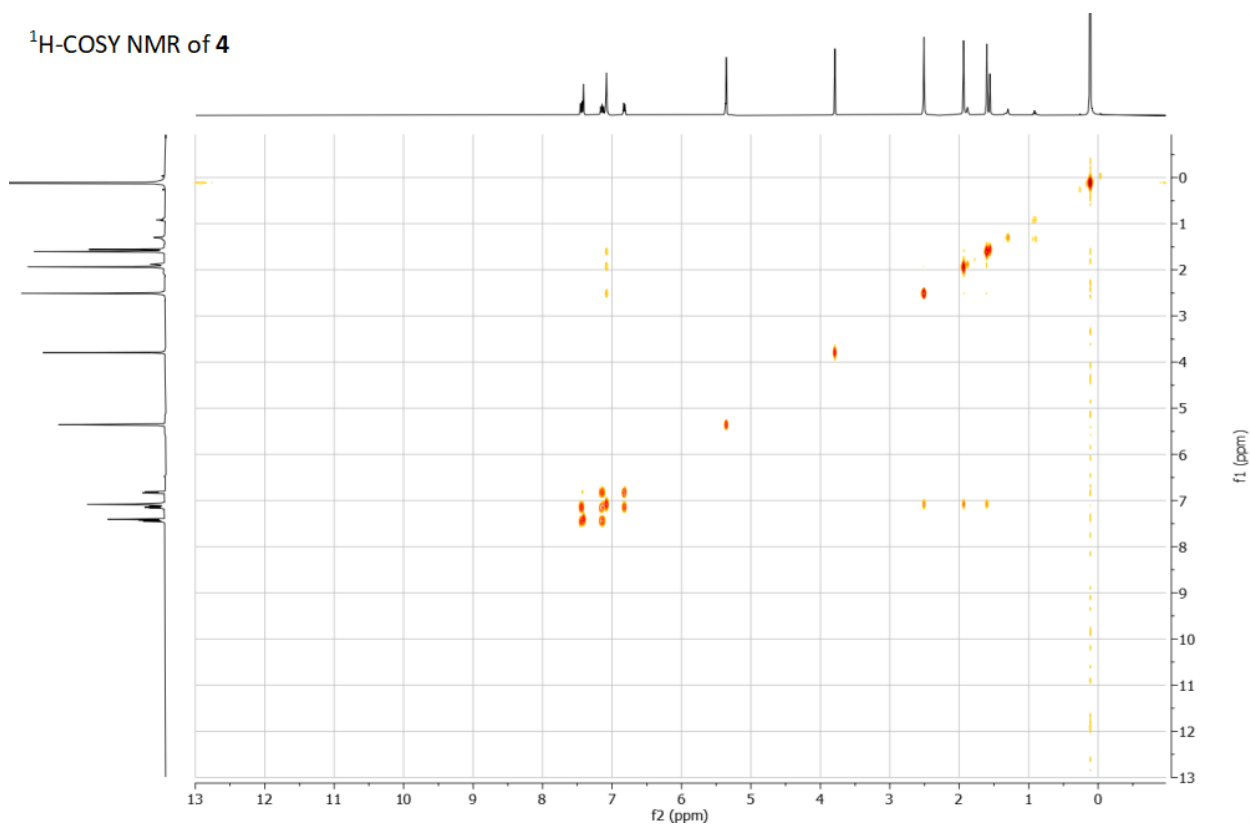


Figure S24. ^1H - ^1H COSY NMR spectrum of **4** (CD_2Cl_2 , 400 / 400 MHz).

Supporting Information

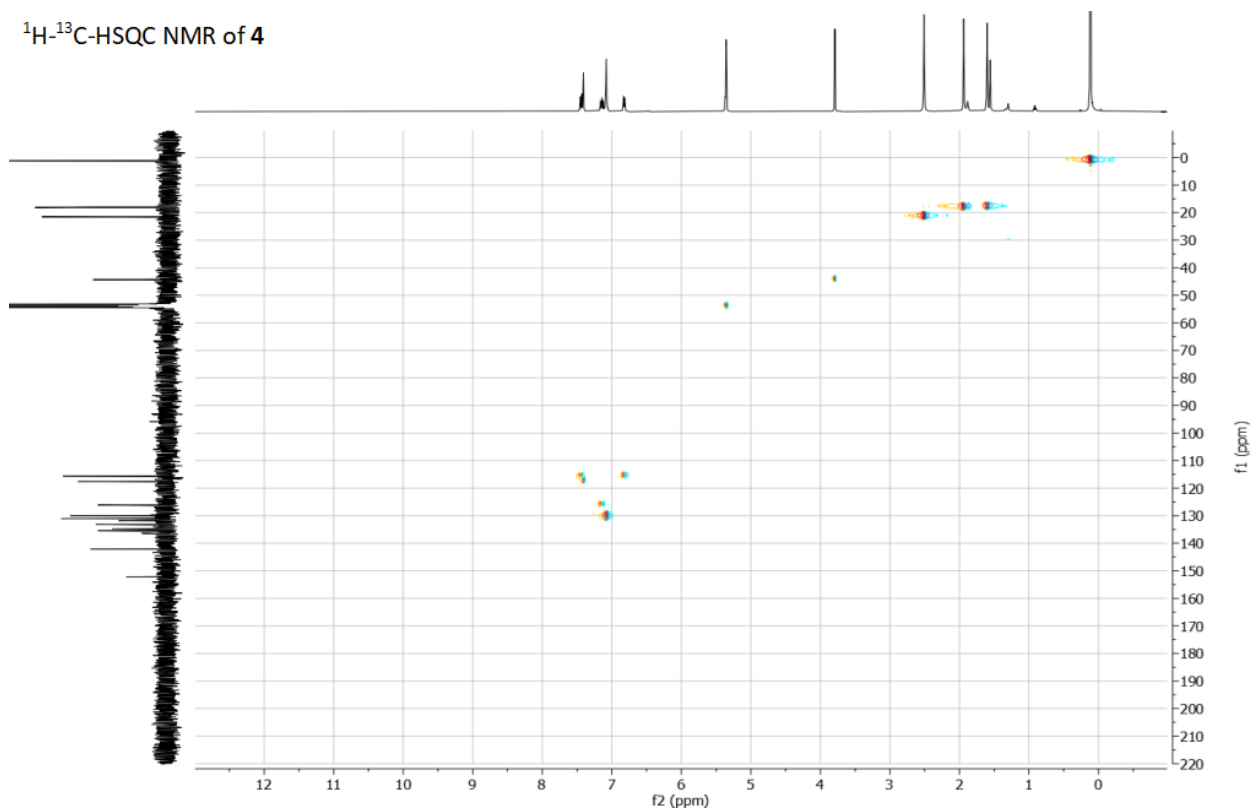


Figure S25. ^1H - ^{13}C HSQC NMR spectrum of **4** (CD_2Cl_2 , 400 / 101 MHz).

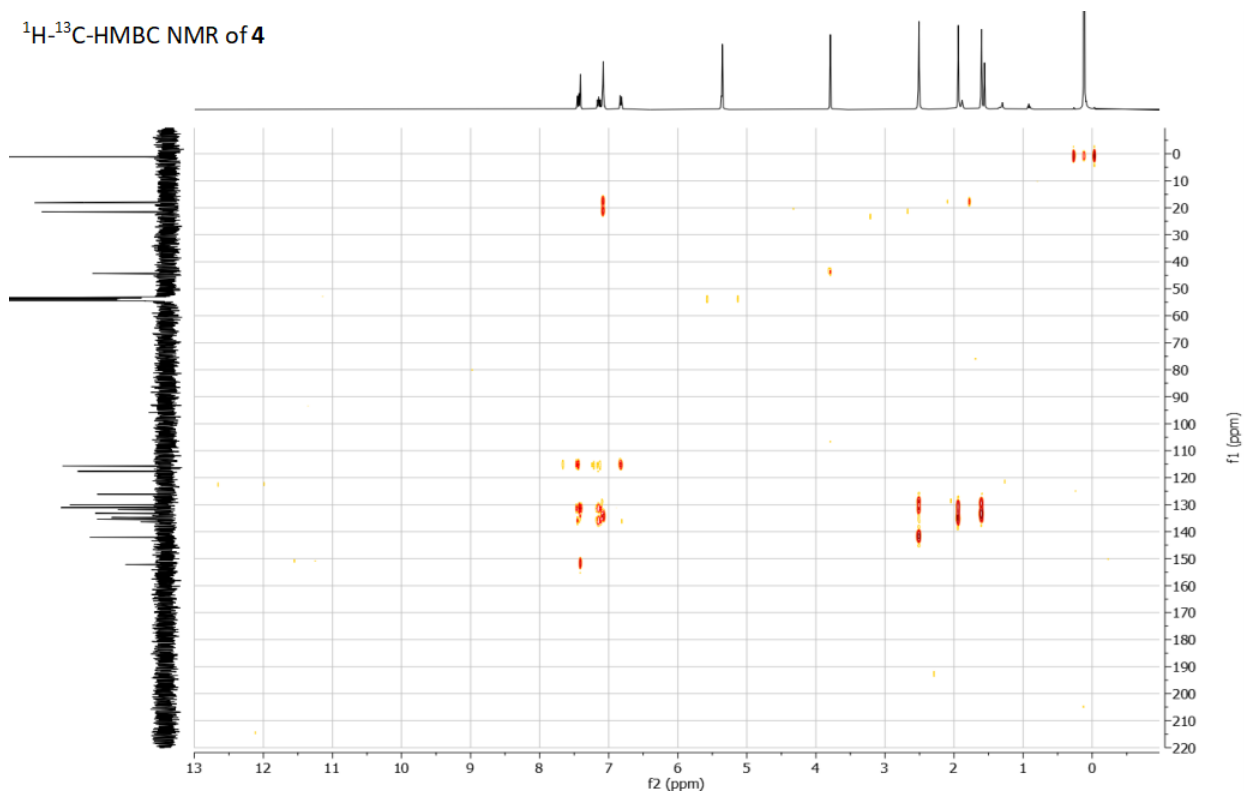


Figure S26. ^1H - ^{13}C HMBC NMR spectrum of **4** (CD_2Cl_2 , 400 / 101 MHz).

Supporting Information

^{19}F NMR of **4**

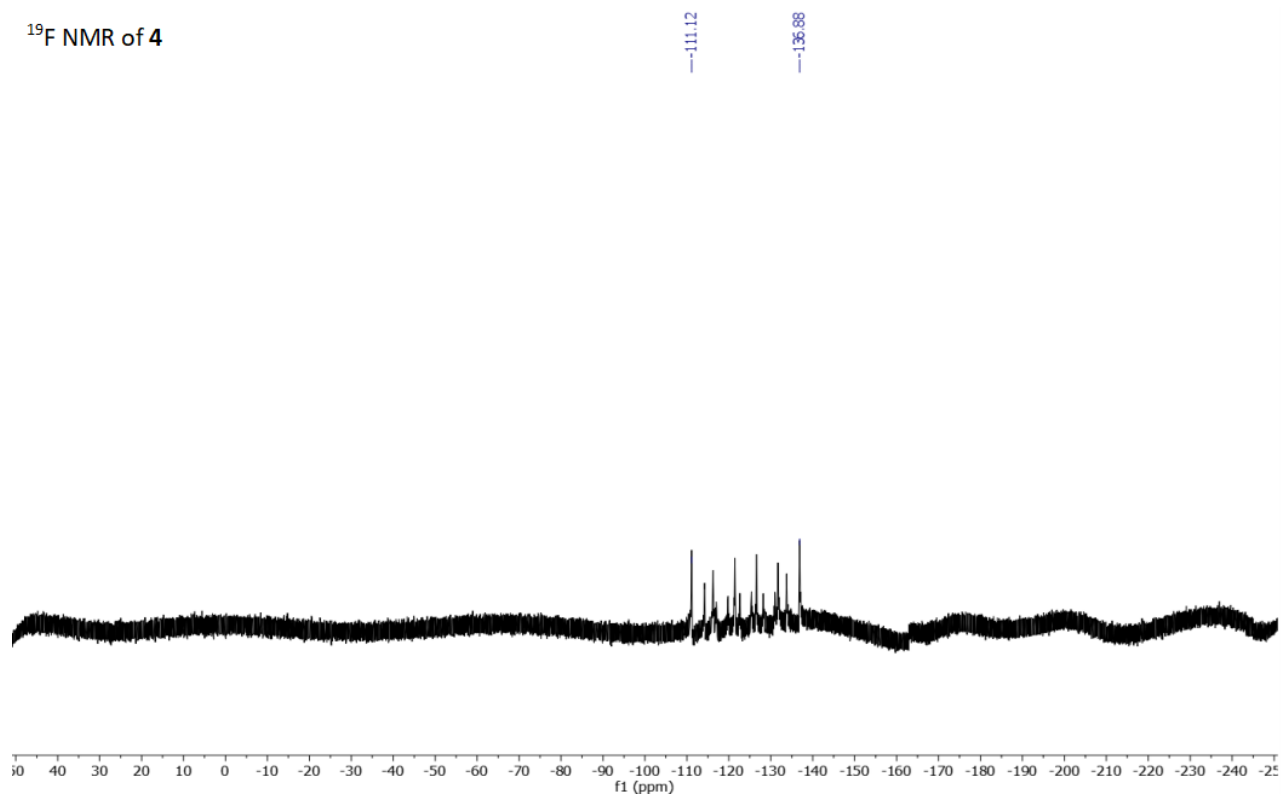


Figure S27. ^{19}F NMR spectrum of **4** (CD_3CN , 376 MHz).

Supporting Information

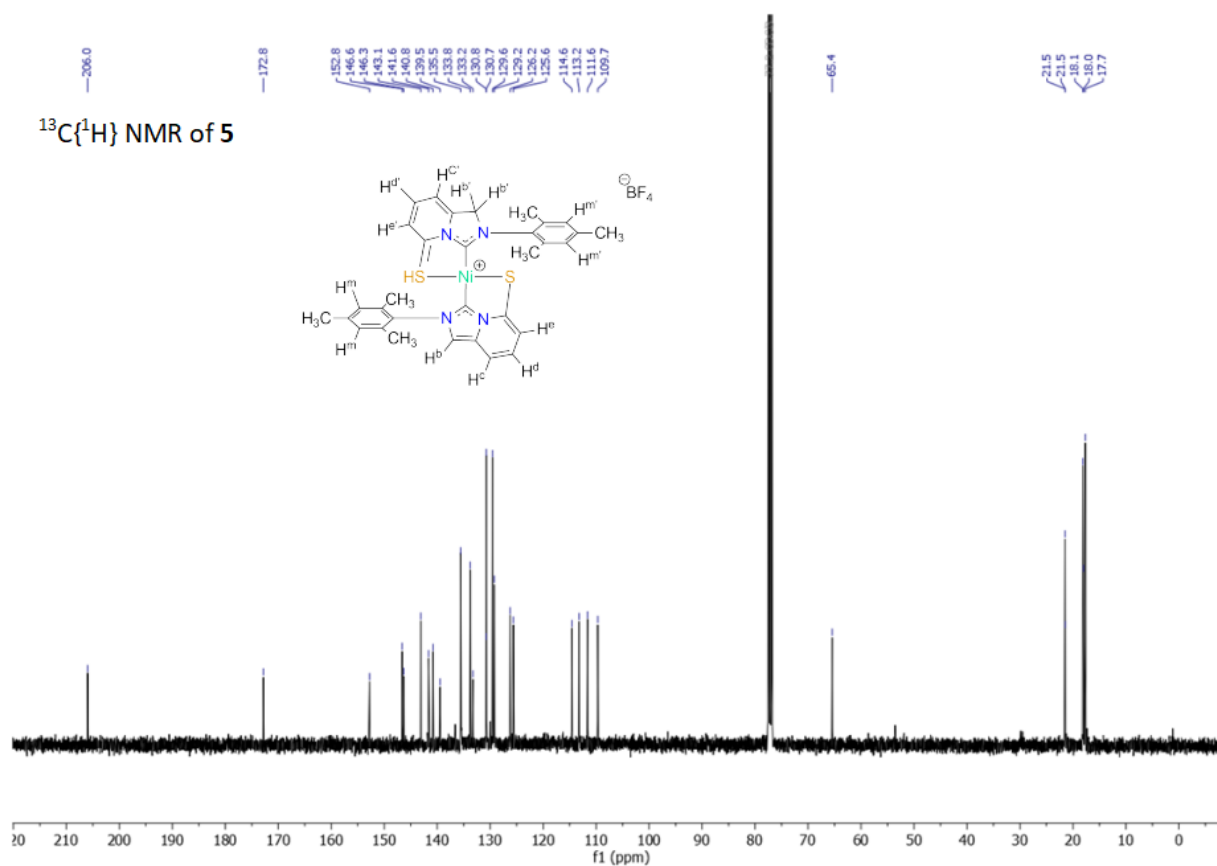


Figure S29. $^{13}\text{C}\{^1\text{H}\}$ NMR spectrum of **5** (CDCl₃, 101 MHz).

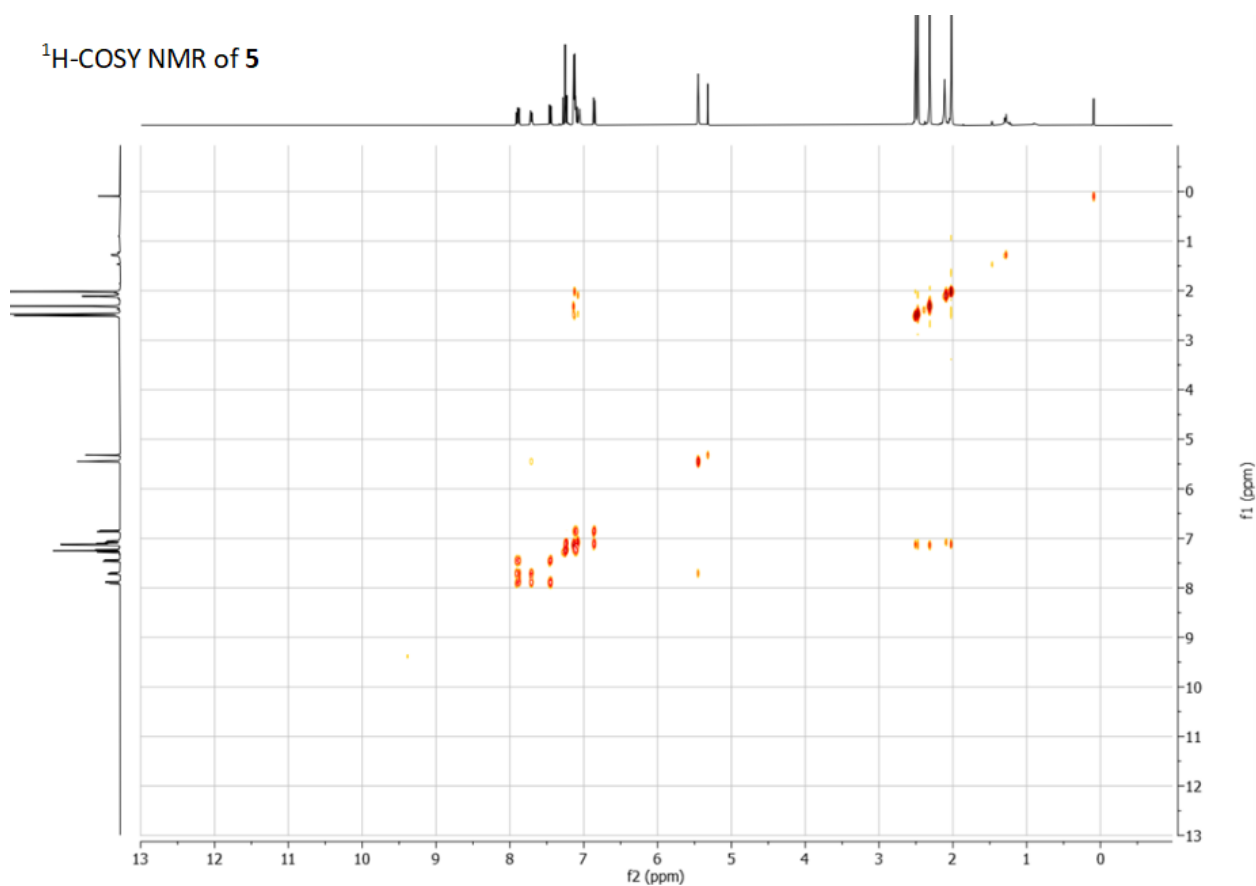


Figure S30. ^1H - ^1H COSY NMR spectrum of **5** (CDCl₃, 400 / 400 MHz).

Supporting Information

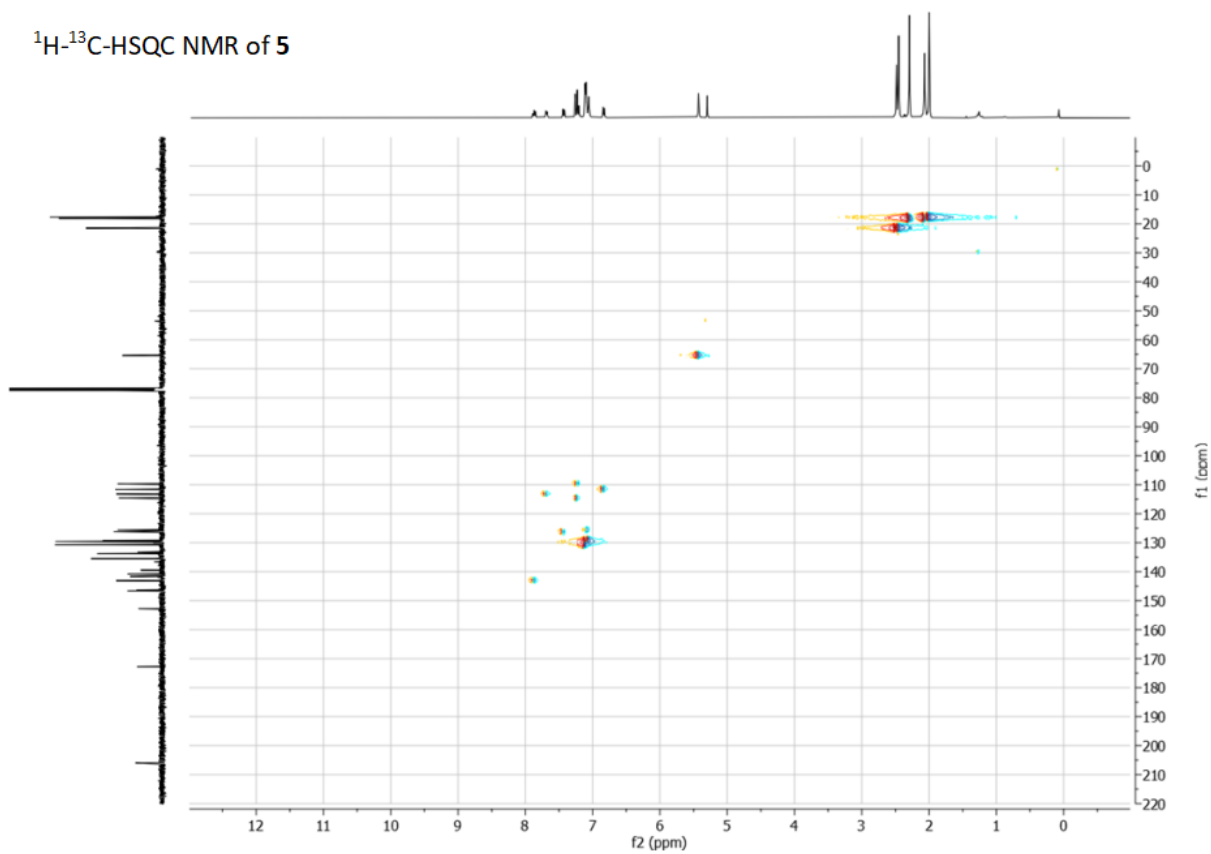


Figure S31. ^1H - ^{13}C HSQC NMR spectrum of **5** (CDCl_3 , 400 / 101 MHz).

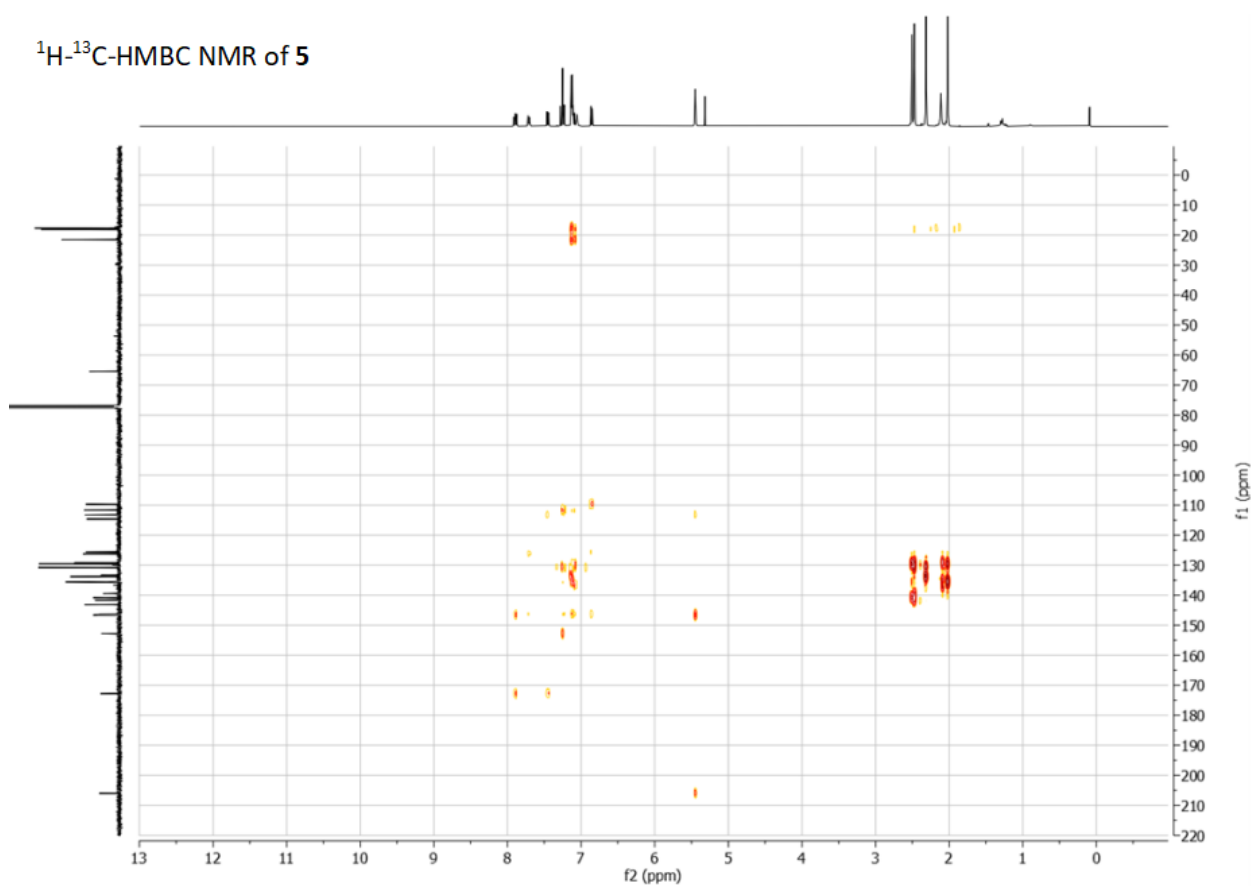
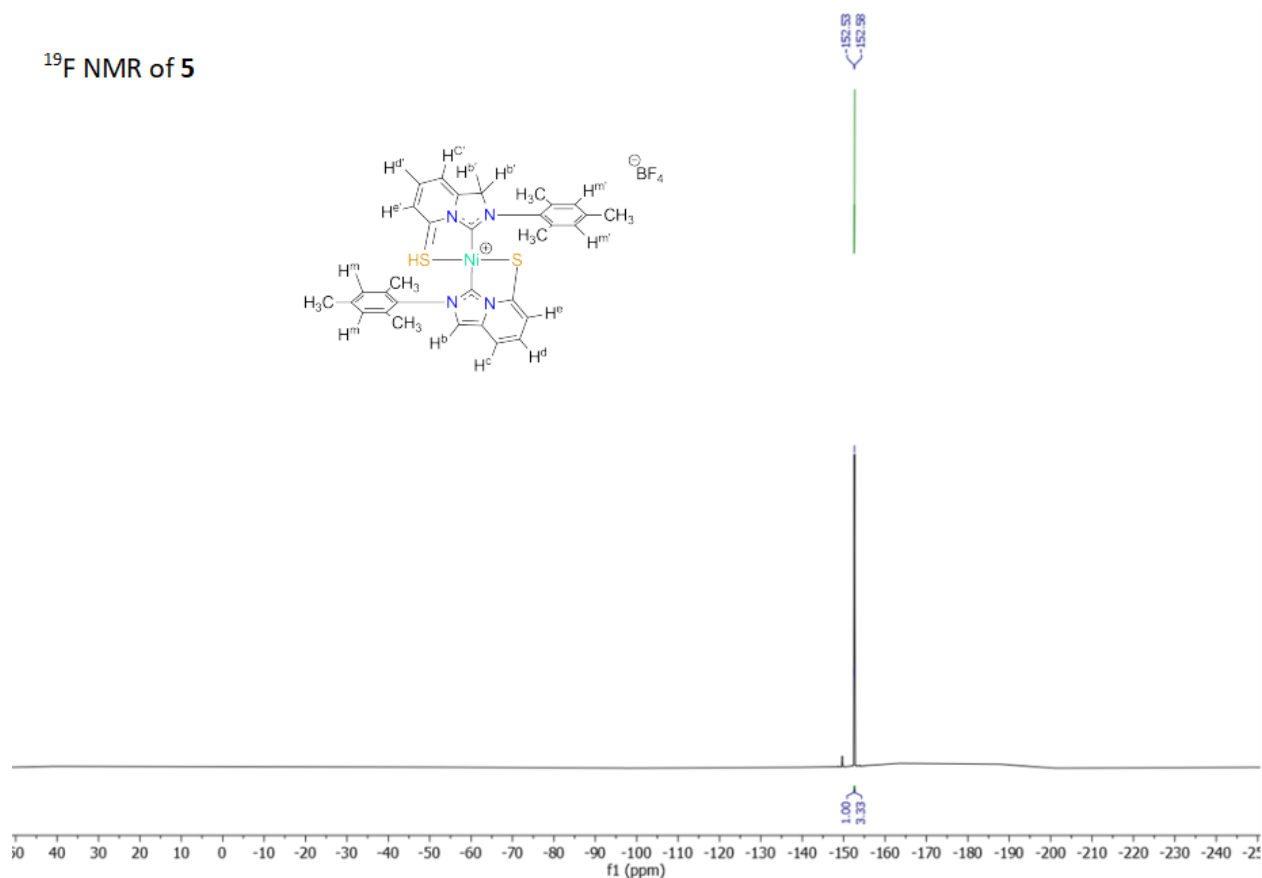


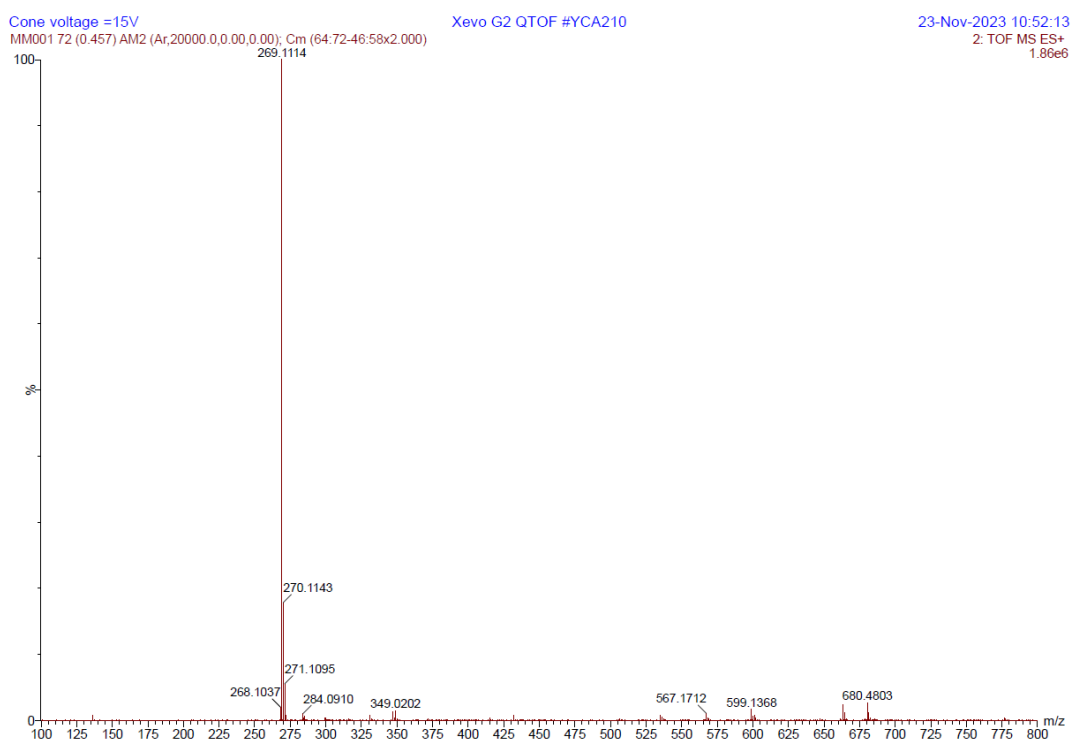
Figure S32. ^1H - ^{13}C HMBC NMR spectrum of **5** (CDCl_3 , 400 / 101 MHz).

Supporting Information

^{19}F NMR of **5**



MS Spectra



Supporting Information

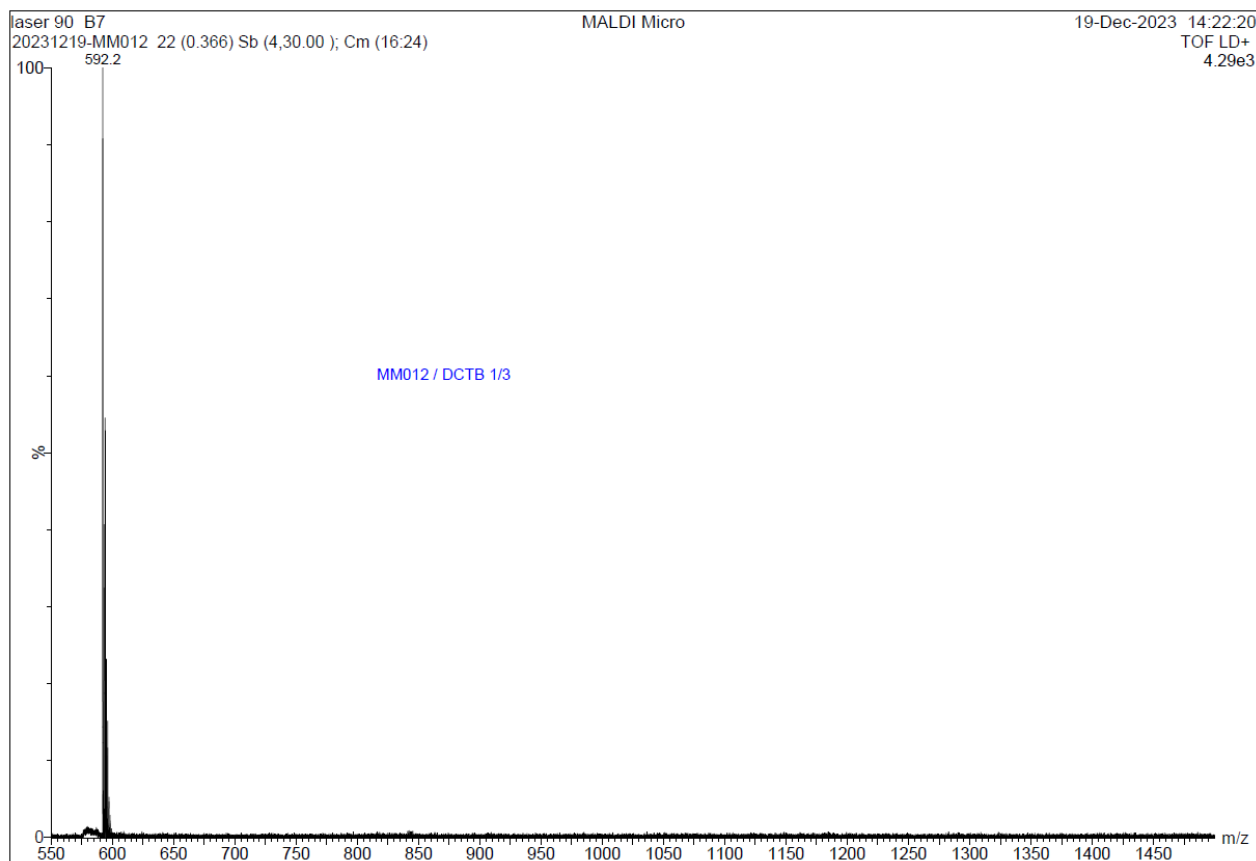


Figure S35. MALDI TOF mass spectrum of **3**.

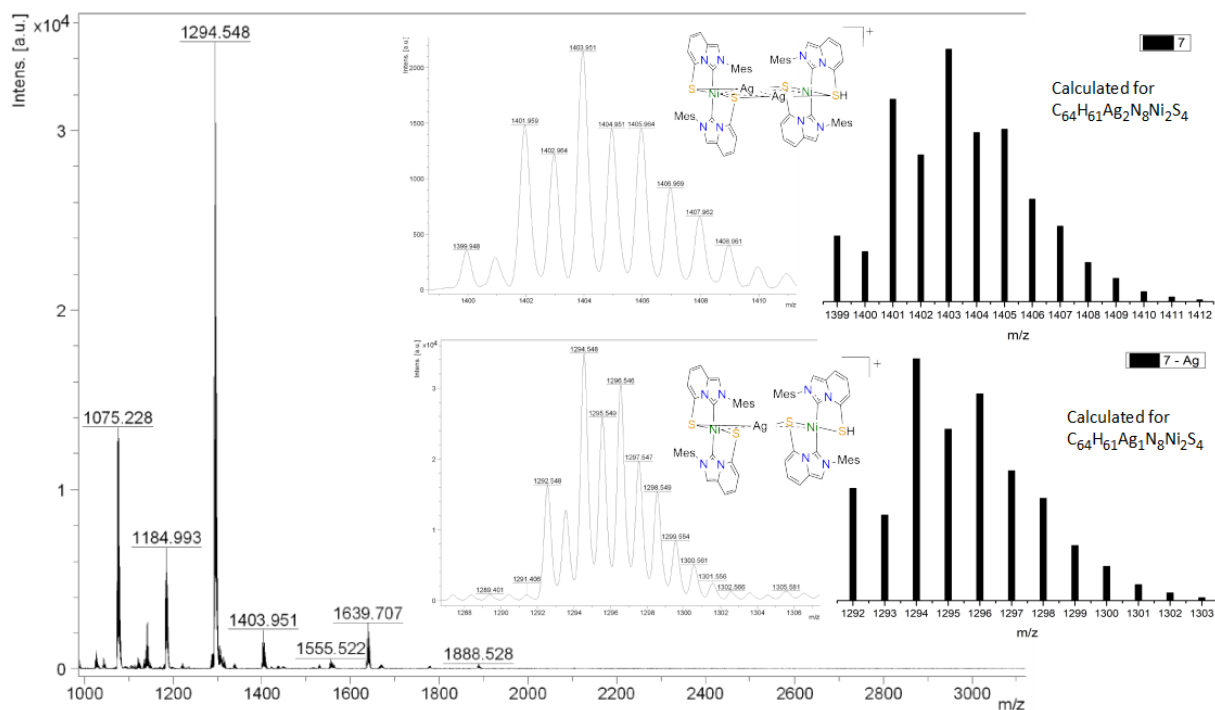


Figure S36. MALDI TOF MS of **4** with comparison of experimental and calculated isotopic patterns.

Supporting Information

UV-Vis spectra of **3**

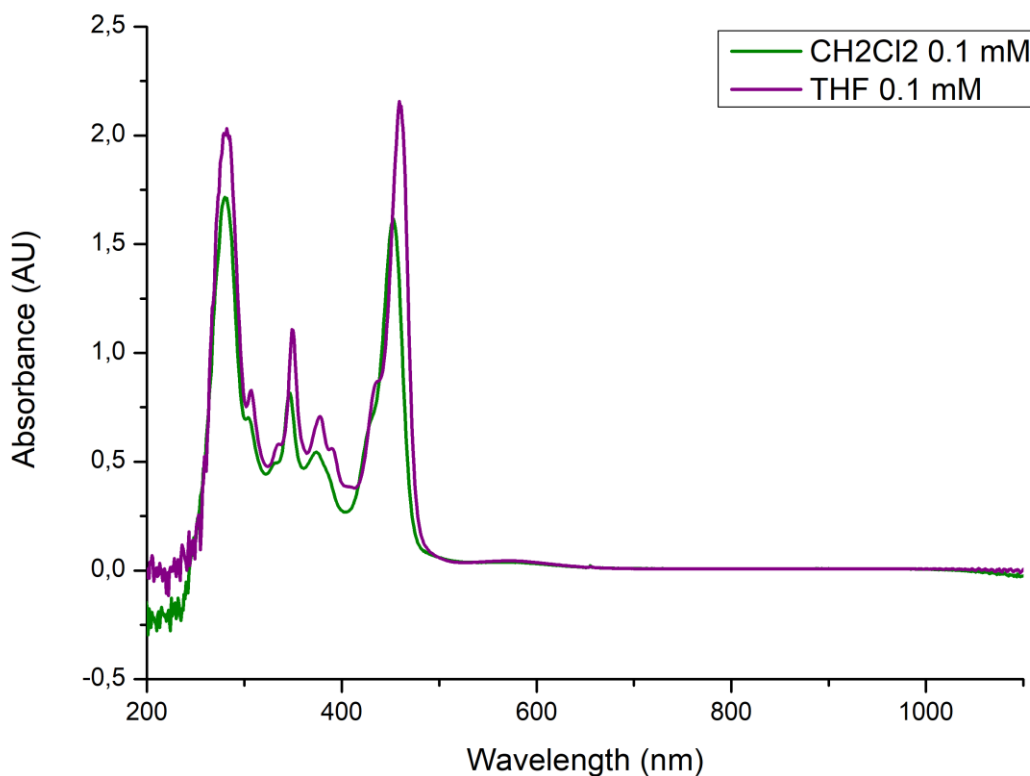


Figure S37. UV-Vis spectra of complex **3** in CH₂Cl₂ and THF

Cyclic Voltammetry

Cyclic voltammetric measurements were carried out with a Autolab PGSTAT100 potentiostat controlled by GPES 4.09 software. Experiments were performed under argon at room temperature in a homemade airtight three-electrode cell. The reference electrode consisted of a saturated calomel electrode (SCE) separated from the solution by a glass frit. The counter electrode was a platinum wire of ca. 1 cm² apparent surface. The working electrode was a Pt microdisk (0.5 mm diameter). The supporting electrolyte, [n-Bu₄N](PF₆) (99% electrochemical grade), was dried at 120 °C and stored under Ar. The CH₂Cl₂ solution of **3** used for the electrochemical studies was 10⁻³ M in complex and 0.1 M in supporting electrolyte. Before each measurement, the solutions were degassed by bubbling Ar and the working electrode was polished with a polishing machine. Potentials are referenced to the SCE, and were calibrated using the Fc⁺/Fc couple by adding ferrocene (10⁻³ M) at the end of the experiments. Under the experimental conditions employed in this work, the half-wave potential (E_{1/2}) of the Fc⁺/Fc couple in CH₂Cl₂ occurred at E_{1/2} = 0.46 V vs. SCE.

Supporting Information

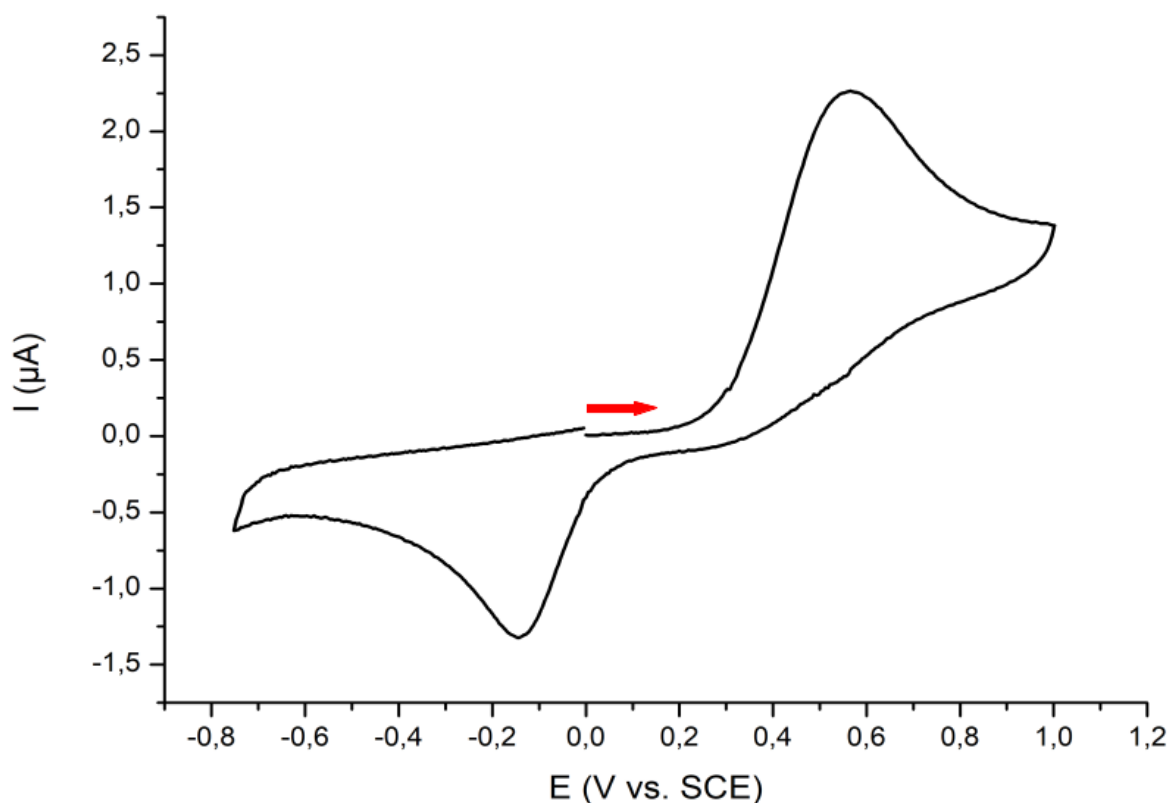


Figure S38. Anodic cyclic voltammogram (CV) of **1·H** (glassy carbon working electrode, 1 mM in CH_2Cl_2 with 0.1 M $[\text{n-Bu}_4\text{N}](\text{PF}_6)$ as the supporting electrolyte, 200 mV s^{-1} scan rate, potentials were calibrated against Fc^+/Fc used as internal standard with $E_{1/2}(\text{Fc}^+/\text{Fc}) = 0.46 \text{ V vs. SCE}$).

DFT calculations

DFT methodology. DFT geometry-optimization of complex **3** (+1 charge, spin $\frac{1}{2}$) has been performed with the ADF code¹⁰ using triple-zeta basis sets combined with the Generalized Gradient Approximation (GGA) VBP exchange-correlation (XC) potential [VWN + BP: Vosko, Wilk & Nusair¹¹ + corrective terms by Becke¹² for the exchange, and Perdew¹³ for the correlation] and ADF grid precision 6. The complex has been embedded within a solvent (DCM) modeled with the COSMO (COnductor-like Screening MOdel)¹⁴ ADF module representing the solvent as a dielectric continuum to mimic an average reaction field response of the environment.

For the computation of the g-tensor, we relied on the PBE0 exchange-correlation potential (25% HF exchange) devised by Ernzerhof-Scuseria¹⁵ and by Adamo-Barone¹⁶. We activated the relativistic (full spin-orbit) option combined with TZ2P basis sets for all atoms.

Supporting Information

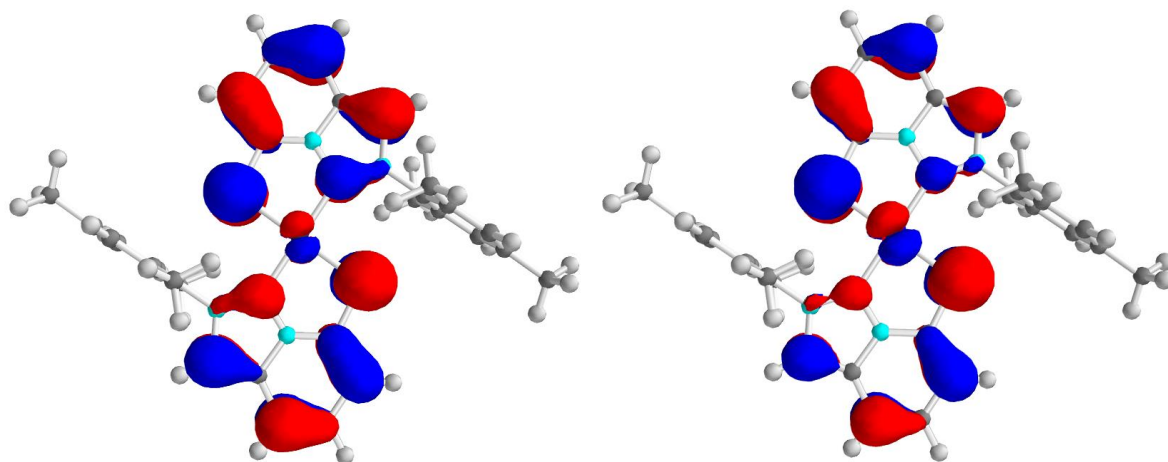


Figure S39. SOMO spin a (left) and corresponding LUMO spin b (right) computed at the VBP XC level (see **DFT Methodology**) with isodensity value set to 0.03 a.u.

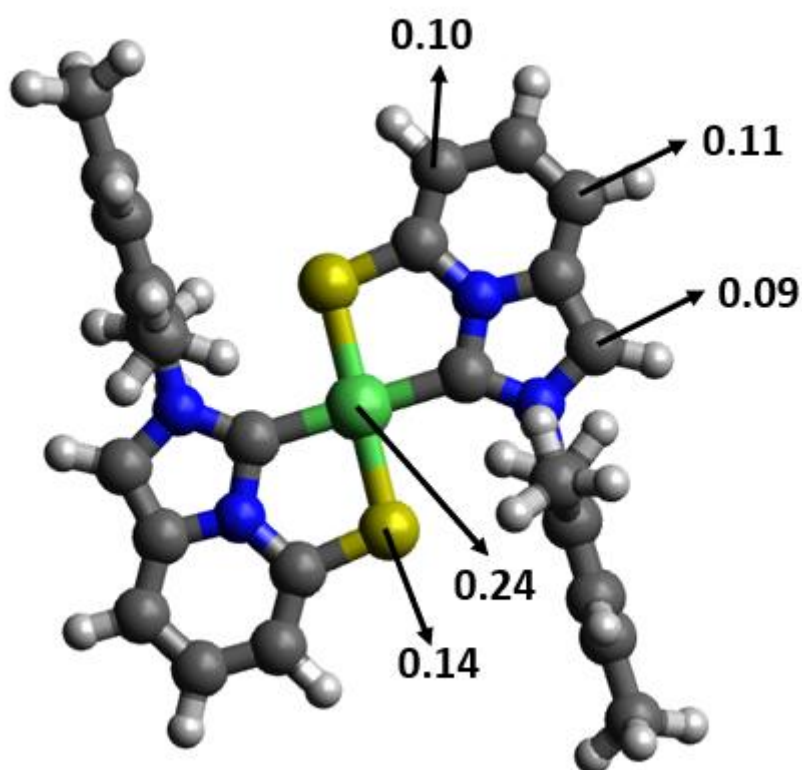


Figure S40. Mülliken spin populations on Nickel (green), Sulfur (yellow) and some Carbon atoms (dark grey) of (3^+). The values on the right ligand are mirrored by those on the left ligand. This yields roughly $\frac{1}{4}$ of the spin population on the Ni atom and the rest is spread over the two ligands (see **Main text**).

References

- ¹ K. Azouzi, C. Duhayon, I. Benaissa, N. Lugan, Y. Canac, S. Bastin, V. César, *Organometallics* 2018, **37**, 4726–4735.
- ² A. Kermagoret, P. Braunstein, *Organometallics* **2008**, *27*, 88–99
- ³ G. R. Fulmer, A. J. M. Miller, N. H. Sherden, H. E. Gottlieb, A. Nudelman, B. M. Stoltz, J. E. Bercaw and K. I. Goldberg, *Organometallics*, 2010, **29**, 2176-2179

Supporting Information

- ⁴ S. Stoll and A. Schweiger, *J. Magn. Reson.*, 2006, **178**, 42-55
- ⁵ G. M. Sheldrick, *Acta Cryst A* 2015, **71**, 3–8
- ⁶ L. J. Farrugia, *J. Appl. Cryst.* 1999, **32**, 837–838
- ⁷ CRYSTALS version 12: software for guided crystal structure analysis - PW Betteridge, JR Carruthers, K Prout, DJ Watkin, *J. Appl. Cryst.* 2003, **36**, 1487.
- ⁸ INTERNATIONAL tables for X-Ray crystallography, 1974, Vol IV, Kynoch press, Birmingham, England
- ⁹ ORTEP3 for Windows - L. J. Farrugia, *J. Appl. Crystallogr.* 1997, **30**, 565
- ¹⁰ G. Velde and E. Baerends, Numerical-Integration for Polyatomic Systems. *J. Comput. Phys.* 1992, **99**, 84
- ¹¹ S. H. Vosko, L. Wilk, and M. Nusair, Accurate Spin-Dependent Electron Liquid Correlation Energies for Local Spin Density Calculations: A Critical Analysis. *Can. J. Phys.* 1980, **58**, 1200
- ¹² A. D. Becke, Density-Functional Exchange-Energy Approximation with Correct Asymptotic Behavior. *Phys. Rev. A* 1988, **38**, 3098
- ¹³ J. P. Perdew, Density-Functional Approximation for the Correlation Energy of the Inhomogeneous Electron Gas. *Phys. Rev. B* 1986, **33**, 8822.
- ¹⁴ (a) A. Klamt and G. Schüürmann, *J. Chem. Soc., Perkin Trans. 2*, 1993, 799–805; (b) A. Klamt, *J. Phys. Chem.*, 1995, **99**, 2224–2235; (c) A. Klamt and V. Jonas, *J. Chem. Phys.* 1996, **105**, 9972–9981
- ¹⁵ M. Ernzerhof and G. Scuseria, Assessment of the Perdew.Burke.Ernzerhof exchange-correlation functional. *J. Chem. Phys.* 1999, **110**, 5029
- ¹⁶ C. Adamo and V. Barone, Toward reliable density functional methods without adjustable parameters: The PBE0 model. *J. Chem. Phys.* 1999, **110**, 6158